LIFE CYCLE ASSESSMENT

GEOTHERMAL ENERGY

GA Drilling

As the first European venture capital fund, Planet A relies on its own scientific team to assess the environmental and climate impact of an innovation. Prior to an investment, a life cycle assessment, like this one, is conducted and integral part of the investment decision. All assessments as well as the methodology are published for maximum transparency.

Terminology and abbreviations

CED_f	Cumulative fossil energy demand
CHP	Combined heat and power
CO_2-eq.	Carbon dioxide equivalents
D	Deep (well)
DS	Dry Steam
DF	Double flash
EGS	Enhanced geothermal system
Functional unit	Quantified performance of a product system for use as a reference unit
GSD	Geometric standard deviation (statistical parameter)
GHG	Greenhouse gas
GTE	Geothermal energy (only in the figure in the Summary section)
IEA	International Energy Agency
ISO	International Organization for Standardization
LCA	Life cycle assessment
LCI	Life cycle inventory
max	Maximum (statistical parameter)
min	Minimum (statistical parameter)
NCG	Non-condensable gasses
ORC	Organic Rankine Cycle
PE	Polyethylene
Perc.	Percentile (statistical parameter)
PVC	Polyvinyl chloride
S	Shallow (well)
SD	Standard deviation (statistical parameter)
SF	Single flash
TES	Triple Expansion Systems
TF	Tripe Flash System
Unc.	Uncertainty

Version 1.0 – April 29 2022

GA Drilling

The Slovakian company GA Drilling developed an innovative technology for drilling wells for deep geothermal power plants. The so-called PlasmaBit Drilling uses a plasma created through an electric arc. The technology allows a more cost-effective and faster drilling of deep boreholes required for future (deep) geothermal power plants. The technology enables the construction of such plants world-wide.

Summary

The presented **Life Cycle Assessment (LCA)** evaluates potential changes in **GHG emissions** and **cumulative fossil energy demand (CED_f)** of geothermal energy production. At present, geothermal energy is mostly extracted from hydrogeological features a few kilometers below ground. **Novel drilling technologies allow faster and more feasible drilling of deep geothermal wells**. Combined with new techniques to increase permeability of underground rock (enhancement), deep geothermal power plants unlock a huge potential for providing **baseload energy supply** by allowing the use of hot underground rock without any existing hydrothermal aquifer.

This study evaluates different geothermal power plant types and accounts for the vast range of real world conditions. The functional units are 1 kWh electricity provided by geothermal electric power plants and 1 kWh heat (plus coupled electricity production) provided by combined heat and power (CHP) plants.

The provision of geothermal energy is likely to displace conventional energy supply. **Two scenarios** are used to model the **displacement of conventional power supply**. A parameterized model was used to account for the most likely real world conditions. A Monte Carlo simulation provides results that provide a range of potential net changes in GHG emissions and the CED_f. The evaluation of the potential net changes in GHG emissions and fossil energy demand reveal that geothermal energy provision can lead to a **substantial reduction in GHG emissions and fossil energy demand exceeding 1 kg CO_2-eq. and 10 MJ per kWh_{el} and kWh_{th}.** All assessed geothermal power plants exhibit a much better environmental performance compared to current conventional energy supply. The displacement of the latter is likely to result in the reported net decreases.

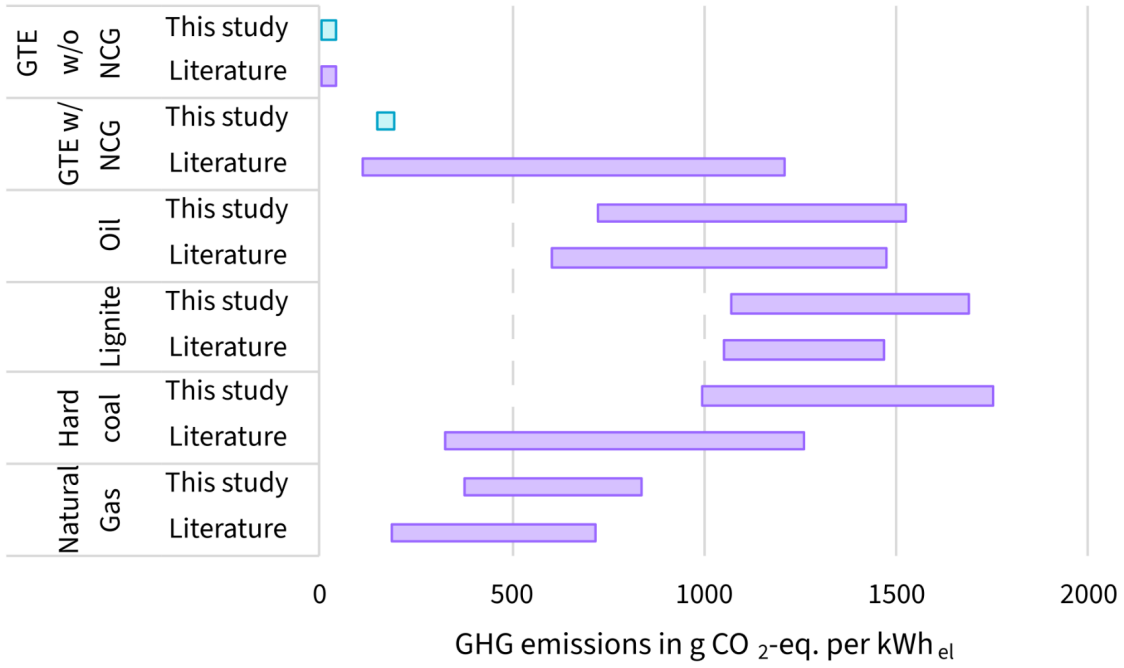

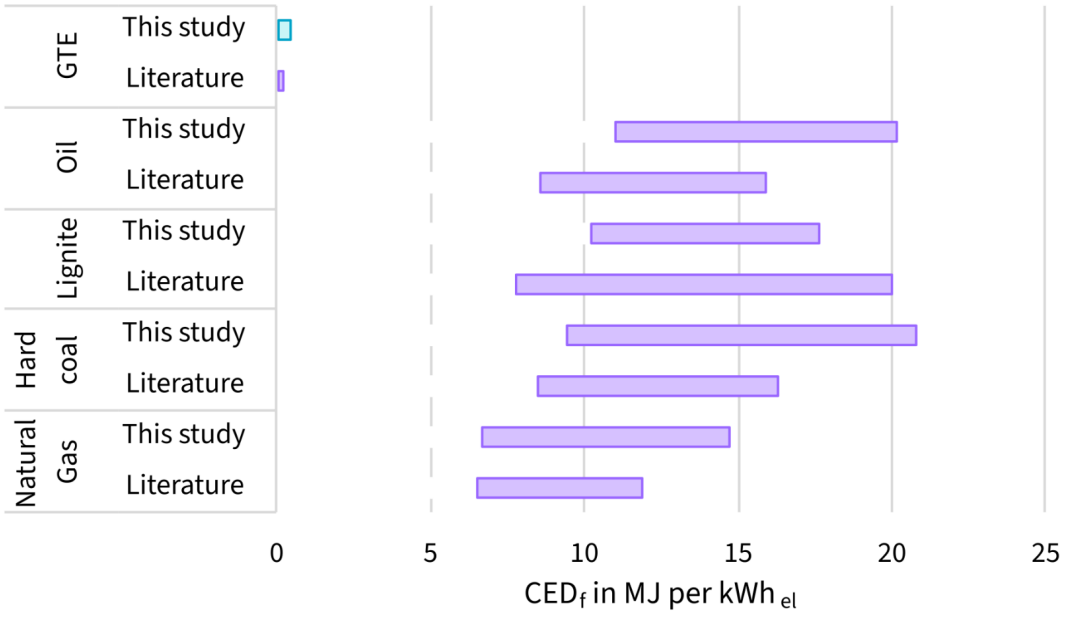

Comparison of GHG intensity and CED_f of geothermal and conventional electricity provision. *Please see the corresponding chapters below for a detailed description of modeled geothermal power plant types and conventional power generation. Values depicted from this study refer to the 5 and 95% percentiles derived from a Monte Carlo Simulation. Literature values were taken from (Tomasini-Montenegro et al. 2017; Menberg et al. 2016; Sullivan et al. 2013; Lacirignola et al. 2014; Parisi et al. 2019; Hondo 2005; Karlsdóttir et al. 2020 (includes values of literature stated in these studies). Abbr.: GHG - Greenhouse gas emissions; GTE - Geothermal energy; NCG - Non-condensable gasses.*

Table of content

1. About this study

This is a summary report of a detailed LCA study evaluating the potential environmental impacts of geothermal energy production. The LCA study is conducted in accordance to the ISO 14040 and 14044 standards[1] for LCA. A consequential LCA approach is applied to evaluate the change in environmental indicators as a result of an increase in electricity and heat production from geothermal power plants. The approach evaluates marginal changes within the overall economy as a consequence of a change in the market structure (e.g., energy supply by geothermal power plants), production modalities, demands as well as political, consumer or any other decision affecting the former aspects (Ekvall et al. 2016).

GA Drilling provides an enabling technology that facilitates the construction and operation of noval geothermal power plants, so-called *enhanced geothermal systems* (EGS). These geothermal power plants can be used in different environmental settings to provide specific energy needs (electricity and heat). The design and performance of the geothermal power plant depends on many local factors. This study seeks to provide an estimation of potential impacts. It is strongly emphasized that potential future geothermal power plants can be designed and operated in a myriad different ways depending on local environmental conditions and the demand for electricity and heat. The local environmental conditions, such as geological features, thermal gradients, etc. and the demand will determine the type of power plant (binary power plants, flash power plants, dry steam plants etc.), the number and depth of wells, and the requirements of additional stimulation (hydrothermal vs. pedothermal systems). Pedothermal systems require additional fracturing.

Please note: It is not possible to consider all power plant designs on all potential markets. This study seeks to provide an estimate of the potential range of environmental impacts according to defined parameter ranges and distributions. The applied approach follows the model developed by (Lacirignola et al. 2014). Please see section 2.2 to 2.4 as well as the Annex for a detailed description of all parameters and formulas.

It is also important to emphasize that GA Drilling provides a technology that enables deep geothermal energy provision. **This study evaluates the environmental performance of such deep geothermal energy production.** In this study, environmental impacts/benefits are not allocated to GA Drilling specifically (or any other party involved in the use and provision of

[1] EN 14040:2006 + AMD 1:2021 (Deutsches Institut für Normung e. V. n.d.) and ISO EN 14044:2016 + AMD 1:2018 + AMD 2: 2020 (Deutsches Institut für Normung e. V., n.d.).

geothermal energy). The purpose of this study is to gain a deeper understanding of the potential overall impact to which GA Drilling can contribute to.

2. System description

The evaluation comprises the full life-cycle of energy provision from geothermal power plants (Figure 1). Aside from the environmental impact of providing electricity and heat, an increase in geothermal power provision will likely substitute existing energy provision. Statistics and scenarios of the International Energy Agency (IEA) are used to determine the substituted means of energy provision (section 2.4). The following geothermal power plants are modeled:

- Dry Steam (DS): DS power plants are suitable for vapor dominated geothermal resources. In such cases, the steam is directly used in a steam turbine to produce electricity. Steam leaving the rubine can either be directly emitted to the atmosphere or condensed (and re-injected).

- Single Flash (SF): in an SF geothermal power plant, the geofluid is directed into a separator in which a decrease in pressure results in a rapid vaporization of steam. The steam is directed to a steam turbine. The remaining liquid can either be used for heating purposes or be directly re-injected into the reservoir. Likewise, (condensed) steam can be optionally used for heating purposes.

- Double Flash (DF): the DF geothermal power plant comprises another flash stage to which the liquid phase of the first flash stage is directed to. Steam from both separators is used to generate electricity in a steam turbine. Remaining heat can be used for heating purposes.

- Binary: A binary power plant comprises two separated heat cycles. The geothermal fluid is cycled through the first cycle. A heat exchanger is used to transfer heat from the first cycle to the second cycle containing a working fluid. The working fluid vaporizes and the steam is used to produce electricity in a turbine. The most common type of binary geothermal power plant are Organic Rankine Cycle (ORC) power plants. Usually, ORC plants are used at lower temperature ranges (<200°C) with low vapour production.

Geothermal power plants can also be designed by combining these principles, e.g. brine bottoming binary systems or spent steam bottoming primary system, or adding additional separators, e.g. triple flash (TF) or triple expansion systems (TES). TES are used at supercritical conditions (i.e. high temperatures and pressures).

Aside from electricity, all of these plants can provide heat. Heat can be obtained after electricity generation or from geothermal fluid streams that are directly used for heating purposes. Again, a large variety of potential plant designs could be developed according to local site characteristics and energy requirements. Today, the most commonly used geothermal power plants are DS, SF, DF or binary power plants. **In this study SF, DF and binary plants are modeled.** This selection is justified by the estimated potential of deep EGS power and the lack of detailed inventory data for the other systems, e.g. DS. According to Aghahosseini and Breyser (2020), only 12% of the global EGS potential (in depth of up to 10 km) falls within the temperature range of TES (above 350°C) (Aghahosseini and Breyer 2020). Therefore, other plant types might be of higher importance in future. Current trends also show that flash and binary plants became the most dominant plant types in recent years, whereas the relative importance of dry flash plants decreased (Uihlein 2018). It should also be noted that for most other plant types than EF, DF and binary plants, there is a lack of inventory data. In section 3.4 most important limitations are discussed.

In addition to the plant design, geothermal power plants can also be distinguished according to the **type of geothermal resource** used. Today, the most common type of geothermal resource used are hydrothermal resources. In such cases, existing aquifers containing hot/warm water are used as a resource. The use of these resources limits the use of geothermal energy due to the limited availability of suitable aquifers. As an alternative, novel approaches seek to access another resource with very high energy content: hot underground rock. In such a case, no natural aquifer is present (or permeability is low). The rock is fractured in order to achieve the required conductivity. Production and injection wells are used to create a heat cycle.

Almost all power plants that have gone into operation have been hydrothermal power plants. Technological advances are required to tap geothermal resources at higher depth. Accessing these heat reservoirs could provide a sustainable source of energy that could play an important role in the future energy supply. Technological advances include novel drilling techniques that lower the costs and time of drilling deeper wells. This requires new drilling techniques as well as advances in materials used (e.g. higher resistance to high temperatures or mechanical stress). Furthermore, the stimulation of hot rock needs to be improved in order to reach the required hydrothermal conductivities. Advancements in these aspects, driven by companies such as GA Drilling, will enable deep EGS power plants.

Aside from geothermal fluid and steam, non-condensable gasses (NGC) are extracted from the underground. The quantity and composition of NGC depends on many local factors. NGC can be a

mixture of H_2, CH_4, CO_2, N_2, Ar, He and other trace gasses (Fridriksson et al. 2016). Depending on the design, NGC are often released to the atmosphere. In closed loop systems, such as binary power plants, the geothermal fluid and gasses are re-injected. For all other plant types, abatement technologies for different gasses could be employed, cf. (Sigfússon et al. 2018; Parisi et al. 2019).

2.1. Functional unit, system boundaries and assessed indicators

The functional unit of this study is defined as **1 kWh of energy supplied by geothermal power plants**. The evaluation comprises the supply of **electricity and heat from shallow and deep geothermal wells**. The **functional units** assessed are:

- 1 kWh of electricity supplied by geothermal power plants
- 1 kWh of heat supplied by a geothermal CHP plant. The reference unit chosen is heat, but the evaluation includes the coupled production of electricity.

The scope of the evaluation is the **global energy supply**. Therefore, a set of parameters is applied to account for the range of real-world conditions. The supply of geothermal energy eventually **displaces conventional base load supply**. The displacement of the conventional energy supply is based on **scenarios of the International Energy Agency** (IEA). All elements considered are depicted in Figure 1. In this assessment the indicators **climate change** (Intergovernmental Panel on Climate Change (IPCC) 2014) and **cumulative fossil energy demand** (CED_f) (Verein Deutscher Ingenieure (VDI) (ed.) 2012) were assessed.

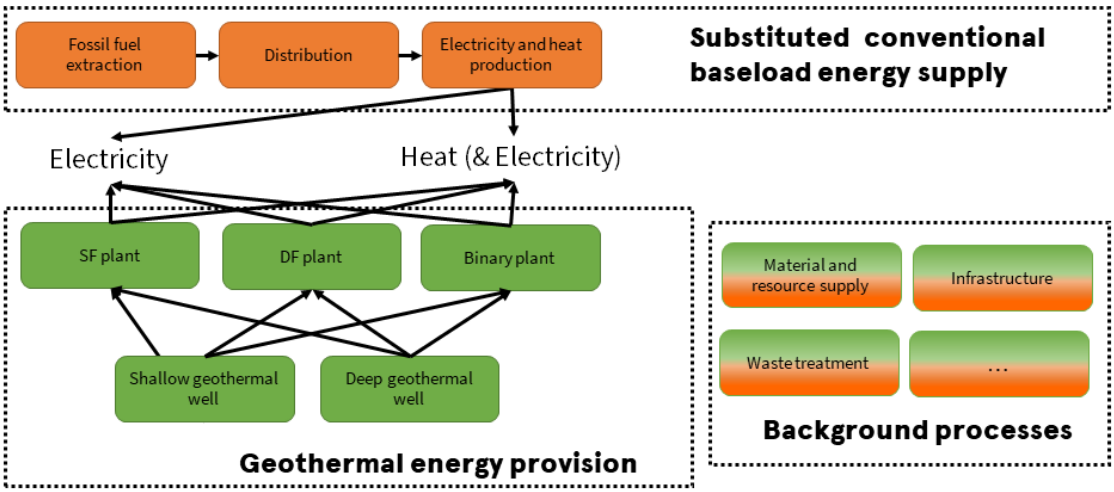

Figure 1 *Depiction of system boundaries. Green processes will commence/increase operation due to geothermal energy provision; orange processes will cease to operate or reduce their production.*

2.2. Modeling approach

Please note: For simplification purposes, the model description refers to GHG emissions. The cumulative fossil energy demand CED_f was assessed analogously (using the CED_f of the supply of all inputs and waste treatment operations).

The model comprises the LCA of geothermal power and conventional power plants, scenarios of geothermal energy and conventional energy supply and the overall evaluation of GHG emissions and the CED_f. Figure 2 depicts where these elements are discussed within this report. First, geothermal and displaced conventional power plants are evaluated individually. Subsequently, energy scenarios and a potential analysis is used to derive supply mixes and to determine the arising displacement effects. The combination of these elements yields the overall net change in GHG emissions and CED_f.

All important characteristics and inventory data are parameterized to account for the vast possibilities of plant designs and local environmental conditions. A Monte-Carlo simulation was conducted with 1000 model runs per power plant.

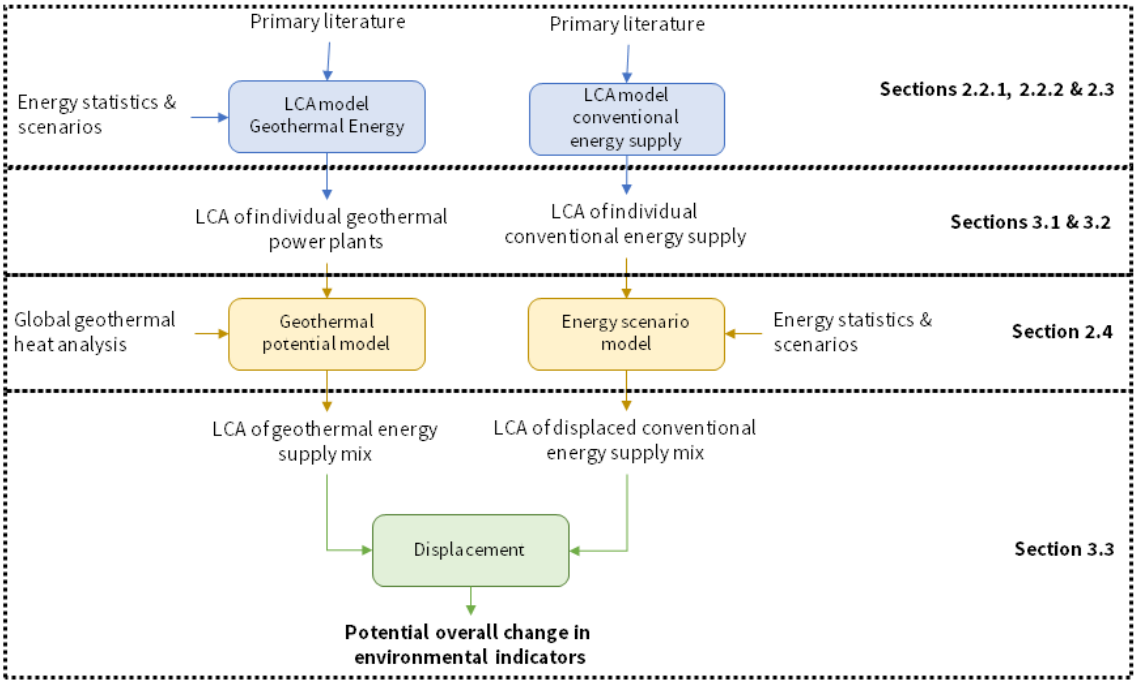

Figure 2 *Elements contained in the evaluation model and report structure.*

2.2.1. Modeling of geothermal power plants

The assessment of potential changes in environmental indicators caused by an increase in geothermal energy production builds on an adapted, generic model developed by Lacirignola et al. (Lacirignola et al. 2014). The original model was built to evaluate binary EGS plants. The model was adapted, additional plant types (i.e. SF and DF) and parameter ranges were included to account for a wider spectrum of potential local site characteristics and energy markets. The model uses a set of parameters and functions to consider different plant types and local conditions without specifying specific site conditions or modeling a geothermal power plant at a specific location. Instead, likely parameter ranges are used to account for the wide range of potential site characteristics. The general structure of all models is expressed in equation (1):

$$GHG_{el} = \frac{GHG\ emitted\ over\ LT}{Energy\ output\ over\ LT} \quad (1)$$

where GHG_{el} are the GHG emissions emitted over the lifetime (LT) of the power plant providing electricity to the grid or heat.

In this study, electricity generation and direct heating use (e.g. district heating and industrial heat) were assessed.

2.2.1.1. Geothermal electricity production

The electricity model comprises two versions: one version for binary plants (adapted version of the model presented in (Lacirignola et al. 2014)) and another model for SF and DF plants. In each model, components are scaled according to the primary literature source. The literature sources also summarize the life cycle inventory (LCI) differently (reporting different components and plant parts representing a sum of plant elements). The modeling of inventory data is described in detail in A.2 of the Annex.

The binary power plant is modeled by an adapted[2] version of the model developed by (Lacirignola et al. 2014):

$$GHG_{el,ORC} = \frac{GHG_{wells}{}^{*}n^{*}d + GHG_{EGS}{}^{*}SF^{*}n + GHG_{ORC}{}^{*}C_{ORC}{}^{*}LT + GHG_{well\ closure}{}^{*}n}{LT^{*}\ LF_{ORC}{}^{*}(1-IPC_{ORC})^{*}C_{ORC-plant}{}^{*}8760} \quad (2)$$

[2] Changes and adaptations to the original model are listed and explained in the Annex.

where the subscripts $wells$, EGS, ORC, and $well\ closure$ a refer to the well drilling and construction of well casing, well enhancement and the ORC infrastructure, operation and maintenance as well as well closing, respectively. The GHG emissions of the components are scaled with the number of wells (n), well depth (d), a scaling factor (SF), the power capacity of the ORC (C_{ORC}) as well as the LT . The load factor (LF), plant's capacity (C) and the internal power consumption (IPC) are considered, too. The chosen binary plant type is an ORC plant.

The SF and DF plants are modeled analogously (equation (3)). The choice of components contained in the model and how they are scaled was adapted according to the available LCI data.

$$GHG_{el,SF/DF} = \frac{GHG_{wells}*n*d + GHG_{EGS}*SF*n + (GHG_{OM} + GHG_{PP,SF/DF})*C_{SF/DF} + GHG_{well\ closure}*n + GHG_{pipelines}*p}{LT*LF_{SF/DF}*(1-IPC_{SF/DF})*C_{SF/D-plant}*8760} \quad (3)$$

In addition to those subscripts already used in equation (2), the subscripts OM, PP, SF/DF, $well\ closure$ and $pipelines$ refer to operation and maintenance, the power plant infrastructure, SF and DF plants, the closing of wells and pipeline construction, respectively. The GHG emissions of the different components are scaled with certain parameters as explained for equation (2) as well as the length of collection pipes (p)[3].

2.2.1.2. Combined heat and power supply

The production of combined heat and power supply was modeled analogously to the electricity supply. In this case, additional GHG emissions of heat supply equipment and materials needed for operation and maintenance were added to equations (2) to (3). The plant capacity and load factors were adapted accordingly.

There are numerous ways how heat can be extracted from the power plant, e.g. serial or parallel heat extraction (Raos et al. 2019; J. Lund and Chiasson 2007). Geothermal power plants can provide heat and electricity in almost all possible ratios. The required ratio depends on local factors, such as local heat and electricity demands. As local future heat and electricity demand cannot be foreseen, it was assumed that geothermal CHP plants fully displace existing conventional CHP plants. Hence, the power to heat ratios were derived from existing and operating conventional power plants (IEA statistics) (Treyer and Bauer 2016). The geothermal CHP plants provide heat and electricity in the same ratio as existing conventional CHP plants. As in all other cases, parameter

[3] Collection pipelines are one example on how the two main literature sources report inventory differently. While pipelines are separately reported in the SF/DF model, they are included in the ORC infrastructure in the binary system model.

ranges were used to account for the diversity of existing conventional CHP plants. **The results of individual CHP plants (i.e. SF, DF and ORC) are presented per kWh of heat produced (kWh_{th}). These results imply the provision of a corresponding amount of electricity (based on the power to heat ratio of existing conventional CHP plants).**

Most inventory components are scaled according to their capacity (see section 2.2.1.1 and A.2). Due to this approach, the scaling and, consequently, the GHG emissions of individual geothermal power plants depend on the power to heat ratio of the displaced power plants. Therefore, GHG emissions of individual geothermal CHP plants are presented for different substitution cases, i.e. displacement of hard coal, lignite, natural gas and oil CHP plants.

2.2.1.3. Additional aspects considered in the modeling of geothermal power plants

In addition to these elements contained in equations (2) to (3), the following is considered:

- The disposal of all materials contained in the infrastructure is accounted for in both models by adding the corresponding quantities of waste to be recycled/treated.
- The emission of NGC is considered in the case of SF and DF plants (Table A13 in the Annex).

2.2.2. Modeling of displaced conventional energy supply

Scenarios describing two potential future energy supply mixes were used to derive the marginal displacement of existing conventional baseload energy supply (section 2.4.2.). The conventional supply of electricity and heat and electricity (CHP) were modeled using the ecoinvent database (Treyer and Bauer 2016). All country-specific data sets were evaluated to account for globally existing power plants.

2.3. Life cycle inventory

This section provides a brief overview of the considered components of the LCI. Please see the corresponding sections in the Annex for a detailed description of LCI data sources and calculation procedures. As previously described, parameter ranges are used for most important parameters to account for potential local conditions (geological characteristics, energy demand, political framework, technical developments, energy prices etc.). The LCI and key parameters used are explained for each element contained in equations (2) to (3) in section A.2 of the Annex in detail. The model comprises all life cycle stages of the built infrastructure (Figure 3). The model comprises three different geothermal power plants providing electricity, i.e. SF, DF and a binary ORC plant, as

well as a geothermal plant for direct heat use (Figure 1). In case of the electricity plants, two well types are evaluated: a shallow well (depth <5,000 m) that uses an existing hydrothermal aquifer and an enhanced deep well (5,000 to 10,000 m). The well of the geothermal heat supply is modeled to a depth of up to 6,000 m. The energy required for all construction and decommissioning purposes that are needed is supplied using diesel.

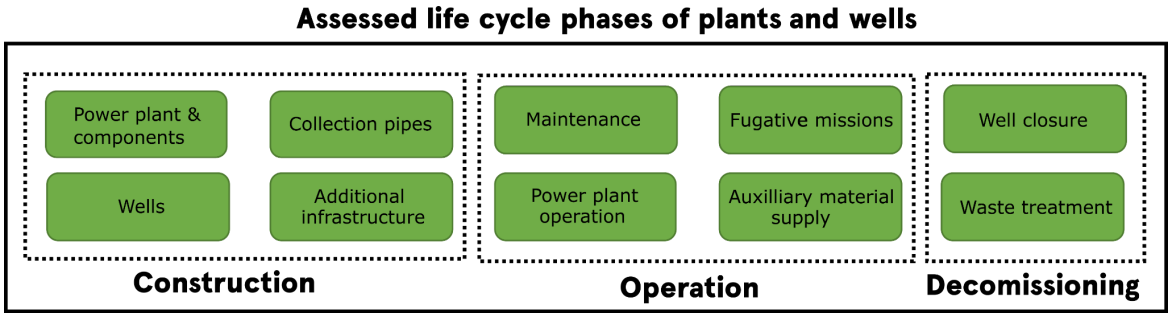

Figure 3 *Elements considered on the assessment of geothermal power plants.*

The conventional supply of electricity and heat and electricity (CHP) were modeled using the ecoinvent database. The interested reader is referred to (Treyer and Bauer 2016) for a detailed description of the inventory of these processes. To account for differences in environmental and technical profiles of power generation in different countries, a total of 371 data sets were evaluated (41 for lignite, 96 for hard coal, 120 for natural gas and 114 for oil) representing electricity generation in different countries and regions within countries. A description of datasets can be found in (Treyer and Bauer 2016).

2.4. Scenarios of geothermal power plants and displaced conventional energy provision

Based on the individual geothermal power plants and existing conventional power plants, GHG emissions and CED_f of geothermal energy supply and conventional energy provision were determined

2.4.1. Geothermal power plant supply scenario

In this study, SF, DF and ORC plants with shallow and deep wells were modeled individually. A potential future energy supply based on these plant and well types was derived from an analysis of geothermal power potential (Aghahosseini and Breyer 2020). Aghahosseini et al. (2020) report the heat content and potential of geothermal power at different depths (Figure 4).

The following principles were applied to obtain the share of each technology:

- Allocation of potential to well depths was accomplished according to well depths of shallow (<5,000m) and deep (5,000 to 10,000m) wells.
- Plant types were selected based on temperature range: ORC plants were considered the most likely plant for the lowest temperature range reported (150-200°C).
- Higher temperature resources were assumed to be accessed by other power plants. It was assumed that each flash plant (SF and DF) each provide half of the geothermal energy supply of the high temperature sources.

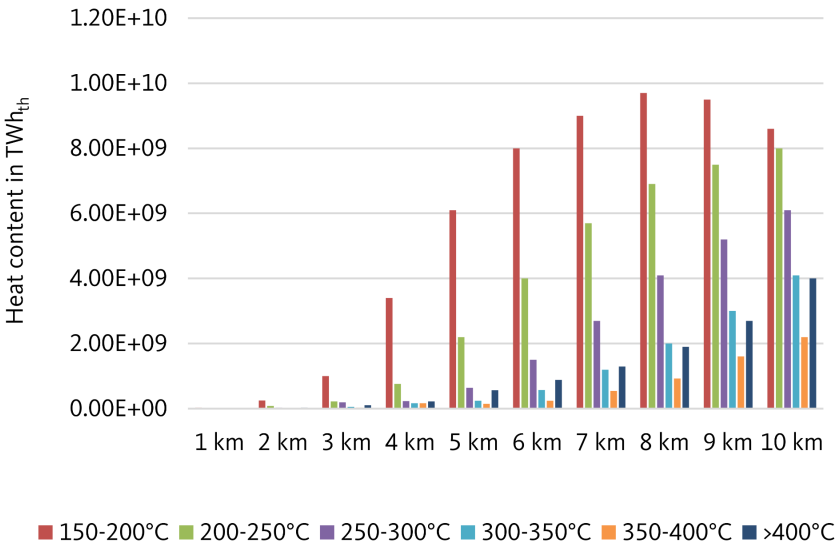

Figure 4 *Extractable heat content at different depths (Aghahosseini and Breyer 2020).*

Table 1 lists the resulting shares of each power plant type. There is a high degree of uncertainty involved in this approach. However, the applied procedure was considered the most feasible and applicable approach. High temperatures allow the utilization of supercritical geothermal systems. Such systems have a higher overall efficiency. To date, no suitable model was available for these type of geothermal power plants. In the limitation section (section 3.4) this approach will be discussed in light of the presented results.

Table 1 *Shares of power plant types in the future geothermal energy supply.*

	SF	**DF**	**ORC**
Shallow	2%	2%	8%
Deep	28%	28%	32%

2.4.2. Displacement of conventional baseload energy supply

At present, baseload energy demand is mainly supplied by conventional, fossil fuel-based energy sources (International Energy Agency 2020). Geothermal energy provides a baseload supply of energy and is therefore not dependent on environmental factors (e.g. wind) nor the day-time (sunlight). It is thus assumed that geothermal energy will penetrate into the market of baseload supply. The two main scenarios of the International Energy Agency's (IEA) World Energy Outlook 2020 assume that the future power generation in the years to 2040 will comprise less coal and oil and less coal, natural gas and oil in the '*Stated policy scenario*' and the '*Sustainable development scenario*', respectively (Figure A3 in the Annex). The projected future energy demand in the power sector was used to derive the share of each energy supply source of the overall decrease in energy supply from the sum of all sources exhibiting a decrease in supply (Table 2 and Table A14 in the Annex). Based on these shares, an average emission factor (and CED_f) was determined corresponding to the decrease in power supply to 2040.

Table 2 *Absolute change in energy supply in the power sector between 2019 and 2040 and share of total decrease. Data source (International Energy Agency 2020).*

	Stated Policy		**Sustainable Development**	
	Absolute change in EJ	% of total decrease	Absolute change in EJ	% of total decrease
Coal	-13.9	80%	-80.39	76%
Oil	-3.56	20%	-6.03	6%
Natural gas			-18.76	18%

A brief note on the IEA energy scenarios: The energy scenarios provide potential energy supply scenarios for the future. The IEA emphasizes that these scenarios are potential developments given a set of assumptions and modeling approaches. Thus, they do not provide a forecast, rather a potential future energy mix if under certain conditions and assumptions. These scenarios help to evaluate the influence of specific decisions and technical developments.

The ***Stated policy scenario*** depicts a potential impact of existing legal frameworks and political announcements. It reflects current plans and presents potential consequences of these plans. The ***Sustainable development scenario*** presents a potential future energy scenario assuming that energy-related Sustainable Development Goals (SDGs) are achieved. It is aligned with the Paris Agreement on Climate Change.

There is no valuation or preordination of either scenario. Both scenarios are evenly likely (among all other potential futures). For further details, please visit https://www.iea.org/reports/world-energy-model.

3. Environmental impact of geothermal energy production

In the following section, the GHG emissions and CED_f of geothermal energy provision is presented. The modeling follows a consequential LCA approach (section 2.2.1). Hence, the presented results reflect the marginal change in GHG emissions and CED_f. This means that results for individual geothermal power plants (section 3.1) and conventional power plants (section 3.2) reflect changes in GHG emissions and CED_f as a consequence of an increase (geothermal power plants) and a decrease (conventional power plants) in demand. In section 3.3. the overall net change in GHG emissions and CED_f is discussed. These results reflect potential marginal changes in GHG emissions and CED_f due to the substitution of conventional baseload energy supply by geothermal energy.

3.1. Geothermal energy production

The average GHG emissions and CED_f of geothermal electricity provision are 13.10 (8.77 to 19.34) g CO_2-eq. and 0.17 (9.11 to 0.26) MJ per kWh_{el}. The GHG emissions and CED_f of geothermal heat provision are 29.20 (14.40 to 53.50) g CO_2-eq. and 0.22 (0.10 to 0.42) MJ per kWh_{th}[4]. All results are presented for individual power plants and for the supply mix in Tables A15 and A6 as well as Figures A3 to A5 in the Annex. The detailed evaluation of GHG emissions and CED_f shows that

[4] These values refer to heat provision in the *Stated policy scenario*. The results of the *Sustainable development scenario* differ only slightly. In case of heat provision, the supply mix depends on the energy scenarios due to the power to heat ratio of existing conventional power plants (see section 2.2.2.2).

power plant infrastructure and well drilling are by far the most important aspects (Figure 5). Well enhancement and well closing does not play a major role in the evaluation. The importance of wells increases with well depth due to more material requirements and energy requirements for drilling. Novel drilling technologies require less energy than conventional contact drilling and the importance of energy requirements for drilling is therefore less pronounced in case of novel drilling technologies, cf. (Menberg et al. 2016). Steel production and processing has the highest impact accounting for more than half of the GHG emissions of well drilling and construction. In this study, steel requirements of 111.3 kg per m were used (Table A2 in the Annex). This is well in line with other studies reporting first hand LCI data (102 and 125 kg per m, (Karlsdóttir et al. 2015; Tosti et al. 2020)). The main contribution to the GHG emissions and CED_f of power plant infrastructure also stems from raw material supply. Due to the higher overall energy output of deep geothermal power plants, the overall impact is lower in case of deep geothermal wells. The results show that most plants have a quite similar environmental profile, if emissions of NCG are excluded. If the emissions of NGC are included, the GHG emissions increase by a factor of 12 (Figure 6). A global average factor of NGC was applied in this study. Literature shows that there is a high variability of the quantity and composition of NCG emissions. These emissions mainly depend on the local characteristics of the rock and geothermal reservoir (Fridriksson et al. 2016). Under certain conditions (volcanic rocks), studies report measured emissions of up to 790 g CO_2-eq. per kWh (Parisi et al. 2019; Fridriksson et al. 2016).

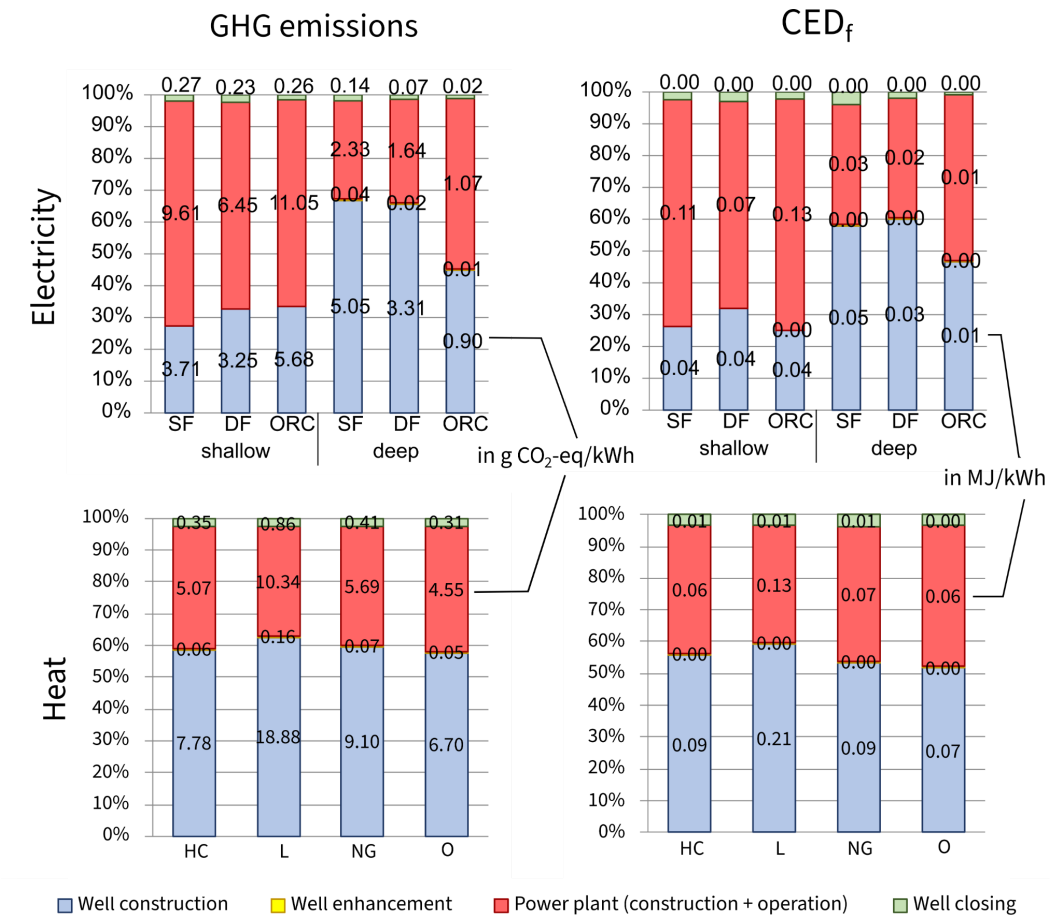

Figure 5 *Average GHG emissions and CED$_f$ of geothermal electricity and heat production (CHP) <u>without</u> emissions of NGC. Abbr. CED$_f$ - cumulative fossil energy demand; DF - double flash; GHG - greenhouse gasses; NCG - non-condensable gasses; ORC - Organic Rankine Cycle; SF - single flash.*

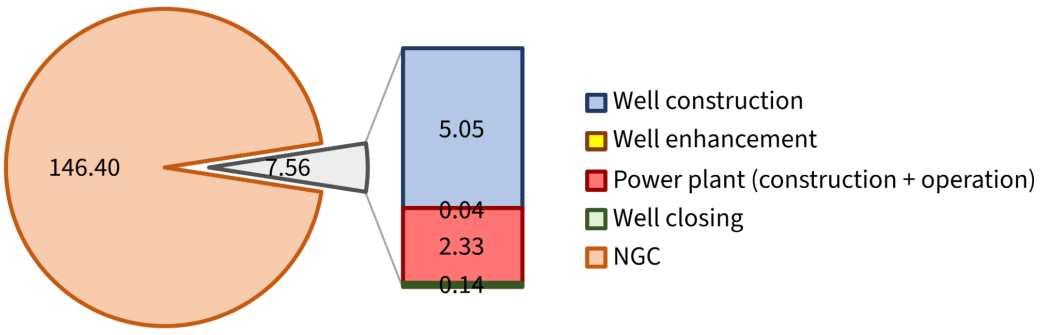

Figure 6 *Detailed GHG emission profile of the SF deep plant including NCG. Abbr. NCG - non-condensable gasses.*

3.2. Displaced conventional energy provision

The GHG intensity and related CED$_f$ of displaced electricity generation is depicted in Figure 7. The GHG intensity and related CED$_f$ of the *Stated policy scenario* and *Sustainable development scenario* were derived from individual GHG emissions and CED$_f$ as well as the power supply reported in the

IEA's 2020 World Energy Outlook (International Energy Agency 2020).

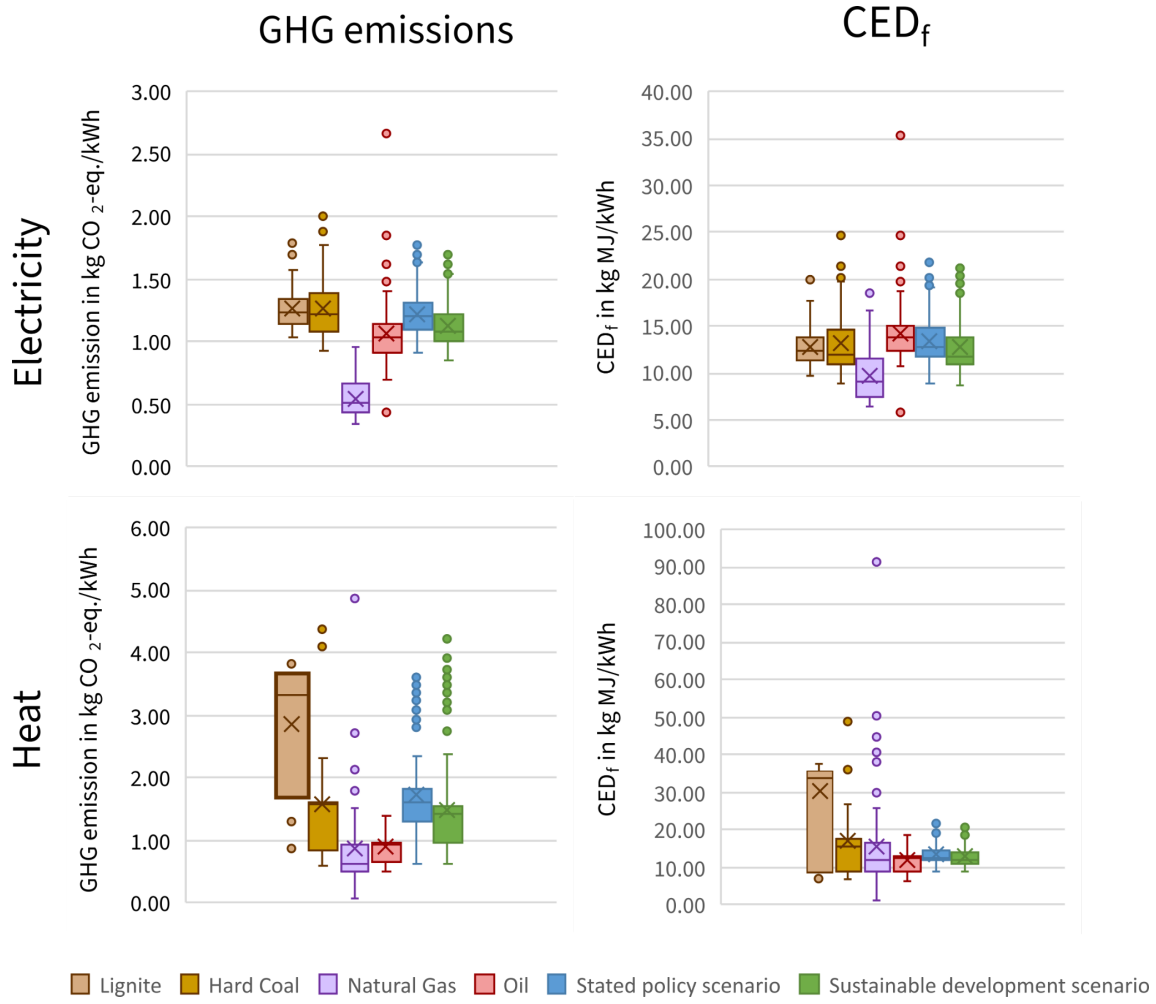

Figure 7 *GHG emissions and CED$_f$ of conventional electricity generation. Evaluated datasets from the Ecoinvent database (Treyer and Bauer 2016). The data sets for lignite, hard coal, natural gas and oil comprise 41, 96, 12 and 114 data sets, respectively. The Stated policy and Sustainable development box plots (and statistical parameters) were defined by random sampling of 1000 datasets (see section A.3 in the Annex for further details). Tables A17 and A18 in the Annex provide all values displayed in the diagram. Abbr. CED$_f$ - cumulative fossil energy demand; GHG - greenhouse gasses.*

The results show that there is only a minor difference in these two scenarios. This is due to the consequential LCA approach that evaluates potential changes in environmental impacts. Therefore, the energy scenarios were used to identify those energy sources and generation methods that will be displaced if geothermal energy penetrates further into the energy market. In both scenarios, coal exhibits the largest absolute (and also relative) decrease in both scenarios. Hence, the GHG intensity and CED$_f$ of both scenarios is dominated by the GHG intensity and CED$_f$ of coal power generation. In the *Sustainable development scenario*, less natural gas is used for energy supply.

Because the reference unit is 1 kWh of electricity, the GHG intensity and CED_f per displaced kWh of electricity is lower in the *Sustainable development scenario* than in the *Stated policy scenario*. It should be kept in mind that there is a much higher absolute decrease in GHG emissions and the use of fossil energy resources in the *Sustainable development scenario.* Thus, per unit of energy displaced, the average benefit is higher in the *Stated policy scenario*, whereas the absolute impact could be (much) higher in the *Sustainable development scenario* as more conventional energy supply is displaced by alternative technologies.

3.3. Overall potential change in GHG emissions and fossil energy demand

The results reveal that the increase in geothermal energy provision potentially results in a substantial reduction in GHG emissions and fossil energy demand exceeding 1 kg CO_2-eq. and 10 MJ per kWh_{el} and kWh_{th} (Figure 8). Detailed results of individual geothermal power plant types (section A.4.3. in the Annex) show that regardless of the geothermal power plant type, substantial reductions are achieved. The lower net reductions in the *Sustainable development scenario* result from the fact that in this scenario, the marginal displacement of fossil fuels comprises natural gas (entailing lower GHG emissions and CED_f than coal and oil). It should be kept in mind that the absolute reduction in GHG emissions and CED_f is much higher in this scenario due to a more stringent displacement of conventional, fossil-based energy generation.

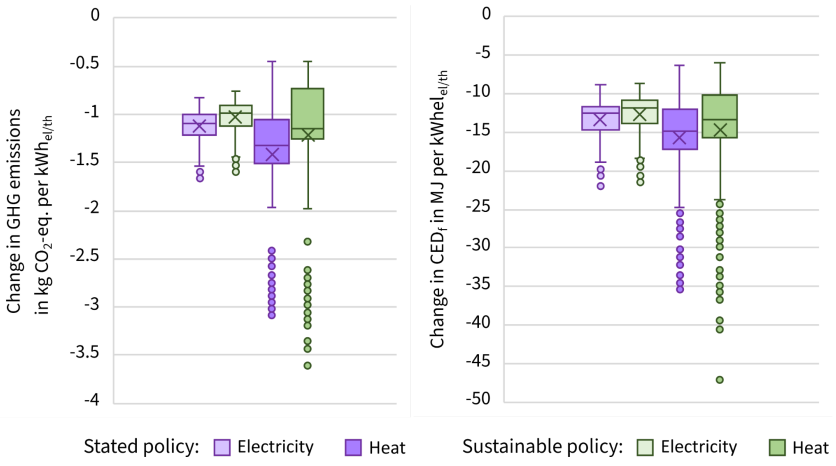

Figure 8 *Net change in GHG emissions and CED_f of geothermal electricity and heat production (CHP). Abbr. CED_f - cumulative fossil energy demand; GHG - greenhouse gasses; NCG - non-condensable gasses.*

3.4. Limitations

The assessment evaluates potential changes in GHG emissions and CED_f as a consequence of the market penetration of geothermal energy. In reality, there is a vast range of environmental

conditions, local energy demands and energy market developments. Additionally, geothermal power plants can be designed and operated in many different ways. To account for a wide range of potential conditions, a parameterized model was developed. The applied approach entails certain limitations, most importantly:

- The parameterized model also implies that certain outcomes of the Monte-Carlo simulation are based on unlikely combinations of parameters. It is not feasible and applicable to build a model that reduces the number of independent variables and includes mathematical relations between these independent variables and all other dependent variables in view of the endless possibilities of all conditions to be considered in such a global analysis. Regardless of the inclusion of some rather unlikely plant set-ups, the presented ranges of potential changes in GHG emissions and CED_f show that net improvements in these impact categories are likely to occur.
- This Study is an evaluation of environmental impacts and does not include the feasibility of geothermal power plants. Certain designs at certain locations are not likely to ever be built. As the endless possibilities of local geological conditions, energy demand, political frameworks and price developments of all alternatives cannot be foreseen, a parameterized approach was chosen. This approach inevitably includes unlikely technical set-ups to a certain extent. However, the overall range that is reported provides an interval that provides insights into potential ranges of environmental impacts. The results demonstrate that geothermal energy results in a net decrease in GHG emissions and CED_f within the applied ranges. Therefore, the confidence in these results is considered high.
- Certain limitations relate to the LCI:
    - LCI data of certain novel drilling technologies is yet not publicly available. Therefore, approximations were used. A wide range of potential energy requirements are applied to account for the uncertainty. Other studies show that energy demand of novel drilling techniques is of subordinate importance in comparison to material use, cf. (Menberg et al. 2016).
    - The LCI is based on a limited number of available studies. To account for uncertainties related to this aspect, wide parameter ranges were selected to include a wide range of potential real world conditions.

- In the case of binary plants, it is assumed that geothermal fluid and steam (including NGC) is re-injected. This approach neglects NGC emission emitted during the exploration and well development phase.
- Abatement technologies for NCG exist. These can lower the GHG emissions (and other pollutants) of geothermal power plants. For example, abatement technologies employed in an Icelandic geothermal power plant reduce GHG emissions by more than 30% (Karlsdóttir et al. 2020). Such technologies were not considered. This is a rather conservative approach as the use of abatement technologies would lower GHG emissions of geothermal power generation.
- Deep wells exhibit high temperatures. This might require other materials than currently used. Due to the lack of inventory data, these could not be modeled. However, the results show a substantial improvement and even (slightly) higher GHG emissions and CED_f will not change the overall outcome of the study
- Deep wells with very high temperatures allow the utilization of supercritical geothermal systems. No suitable parameterized model to assess supercritical geothermal systems was available at the date of the presented assessment.
- These systems require further technical developments of present systems but could also result in a higher efficiency of geothermal power plants (Reinsch et al. 2017). The inclusion of these characteristics is likely to further better the environmental performance of geothermal energy production. Hence, results presented in this study are rather conservative. Conventional power plants: Displaced conventional energy generation is modeled with LCI corresponding to present power plants. This approach can be justified by the fact that these will be the plants that cease operation (in case political commitments will be fulfilled).

- The used energy scenarios are one potential future development. In reality, the energy sector might develop differently than stated in these scenarios. However, if political commitments concerning climate change mitigation will be turned into reality, fossil energy generation will be displaced by renewable energy sources. In consideration of these developments, the presented results would not change much.

4. Conclusion

This study evaluates potential net changes GHG emissions and fossil energy demand of geothermal energy production. **The assessment focuses on shallow and deep geothermal wells**. Novel drilling technologies will make deep geothermal well drilling more feasible and faster. Therefore, a comprehensive understanding of potential environmental impacts is required. To account for the vast possibilities of power plant design, existing conventional energy supply (that is displaced) and environmental factors (e.g. rock characteristics), a parameterized model was developed. Wide ranges of all input parameters were applied in a Monte-Carlo simulation to account for these aspects.

The evaluation of potential net changes in GHG emissions and fossil energy demand reveal that geothermal energy provision can lead to a **substantial reduction in GHG emissions and fossil energy demand** exceeding 1 kg CO_2-eq. and 10 MJ per kWh_{el} and kWh_{th}: the average net reduction is -1.1 and -1.0 kg CO_2-eq. per kWh_{el} in the stated policy and sustainable policy scenario, respectively. The net reduction in fossil energy demand are -13.3 and -12.8 MJ per kWh_{el}.

These numbers show that displacing conventional energy supply by geothermal energy is an effective way to mitigate climate change while supplying base-load energy. The reduction of fossil energy demand is another strong advantage of geothermal energy as it allows to provide electricity and heat at any time at many suitable locations world-wide. Deep wells provide access to high temperature reservoirs making geothermal energy a suitable alternative to conventional energy supply. Deep geothermal energy can therefore support the shift from fossil fuels to renewable energy. Such a shift does not only mitigate climate change, but also increases energy security by reducing the dependency on fossil energy exporting countries.

References

Aghahosseini, Arman, and Christian Breyer. 2020. “From Hot Rock to Useful Energy: A Global Estimate of Enhanced Geothermal Systems Potential.” *Applied Energy* 279: 115769.

Bakema, Guido, and Frank Schoof. 2016. “Geothermal Energy Use, Country Update for The Netherlands.” In *Proceedings of the European Geothermal Congress 2016*,.

Bayer, Peter, Ladislaus Rybach, Philipp Blum, and Ralf Brauchler. 2013. “Review on Life Cycle Environmental Effects of Geothermal Power Generation.” *Renew Sust Energ Rev (Renewable and Sustainable Energy Reviews)* 26: 446–63.

Bertani, Ruggero, and Ian Thain. 2002. “Geothermal Power Generating Plant CO2 Emission Survey.” *IGA news* 49: 1–3.

Blanc, I. et al. 2020. “First Version of Harmonized Guidelines to Perform Environmental Assessment for Geothermal Systems Based on LCA and Non LCA Impact Indicators: LCA Guidelines for Geothermal Installations.”

Boissavy, Christian. 2019. “Report Reviewing Existing Insurance Schemes for Geothermal” ed. Geodeep.

Deutsches Institut für Normung e. V.,. “Umweltmanagement – Ökobilanz – Anforderungen Und Anleitungen.” 13.020.10; 13.020.60(ISO 14044:2006 + Amd 1:2018+ Amd 2:2020).

Deutsches Institut für Normung e. V. “Umweltmanagement – Ökobilanz – Grundsätze Und Rahmenbedingungen.” 13.020.10; 13.020.60(EN ISO 14040:2006 + A1:2020).

Ekvall, Tomas et al. 2016. “Attributional and Consequential LCA in the ILCD Handbook.” *The International Journal of Life Cycle Assessment* 21(3): 293–96.

Fridriksson, Thráinn, Almudena Mateos, Pierre Audinet, and Yasemin Orucu. 2016. *Greenhouse Gases from Geothermal Power Production*. World Bank, Washington, DC.

Hondo, Hiroki. 2005. “Life Cycle GHG Emission Analysis of Power Generation Systems: Japanese Case.” *ECOS 2004 - 17th International Conference on Efficiency, Costs, Optimization, Simulation, and Environmental Impact of Energy on Process Systems 17th International Conference on Efficiency, Costs, Optimization, Simulation, and Environmental Impact of Energy on Process Systems* 30(11–12): 2042–56.

Intergovernmental Panel on Climate Change (IPCC), ed. 2014. *Climate Change 2013 - The Physical Science Basis*. Cambridge: Cambridge University Press.

International Energy Agency. 2020. *World Energy Outlook 2020*. Paris: IEA Publications.

International Finance Corporation. 2013. “Success of Geothermal Wells : A Global Study” ed. World Bank. https://openknowledge.worldbank.org/handle/10986/16493.

Karlsdóttir, Marta Rós, Jukka Heinonen, Halldor Palsson, and Olafur P. Palsson. 2020. “Life Cycle Assessment of a Geothermal Combined Heat and Power Plant Based on High Temperature Utilization.” *Geothermics* 84: 101727.

Karlsdóttir, Marta Rós, Ólafur Pétur Pálsson, Halldór Pálsson, and Larisa Maya-Drysdale. 2015. “Life Cycle Inventory of a Flash Geothermal Combined Heat and Power Plant Located in Iceland.” *The International Journal of Life Cycle Assessment* 20(4): 503–19.

Kocis, I. et al. 2017. “Novel Deep Drilling Technology Based on Electric Plasma Developed in Slovakia.” In *2017 XXXIInd General Assembly and Scientific Symposium of the International Union of Radio Science (URSI GASS)*, IEEE, 1–4.

Lacirignola, Martino, Bechara Hage Meany, Pierryves Padey, and Isabelle Blanc. 2014. “A Simplified Model for the Estimation of Life-Cycle Greenhouse Gas Emissions of Enhanced Geothermal Systems.” *Geothermal Energy* 2(1): 200.

Lowry, T. et al. 2017. “GeoVision Analysis Supporting Task Force Report: Reservoir Maintenance and Development.”

Lund, John, and Andrew Chiasson. 2007. “Examples of Combined Heat and Power Plants Using

Geothermal Energy."
Lund, John, and Aniko N. Toth. 2021. "Direct Utilization of Geothermal Energy 2020 Worldwide Review." *Geothermics* 90: 101915.
Menberg, Kathrin, Stephan Pfister, Philipp Blum, and Peter Bayer. 2016. "A Matter of Meters: State of the Art in the Life Cycle Assessment of Enhanced Geothermal Systems." *Energy & Environmental Science* 9(9): 2720–43.
Parisi, Maria Laura, Nicola Ferrara, Loredana Torsello, and Riccardo Basosi. 2019. "Life Cycle Assessment of Atmospheric Emission Profiles of the Italian Geothermal Power Plants." *Sustainable Development of Energy, Water and Environment Systems* 234(2): 881–94.
Raos et al. 2019. "Multiple-Criteria Decision-Making for Assessing the Enhanced Geothermal Systems." *Energies* 12(9): 1597.
Reinsch, Thomas et al. 2017. "Utilizing Supercritical Geothermal Systems: A Review of Past Ventures and Ongoing Research Activities." *Geothermal Energy* 5(1): 16.
Sanyal, S. K. et al. 2014. "Geothermal Resource Risk in Indonesia–a Statistical Inquiry" ed. World Bank Group.
Sigfússon, Bergur et al. 2018. "Reducing Emissions of Carbon Dioxide and Hydrogen Sulphide at Hellisheidi Power Plant in 2014-2017 and the Role of CarbFix in Achieving the 2040 Iceland Climate Goals." *Energy Procedia* 146: 135–45.
Stefánsson, Valgardur. 2002. "Investment Cost for Geothermal Power Plants." *Geothermics* 31(2): 263–72.
Sullivan, J. L. et al. 2013. "Cumulative Energy, Emissions, and Water Consumption for Geothermal Electric Power Production." *Journal of Renewable and Sustainable Energy* 5(2): 023127.
Tomasini-Montenegro, C. et al. 2017. "Life Cycle Assessment of Geothermal Power Generation Technologies: An Updated Review." *Applied Thermal Engineering* 114: 1119–36.
Tosti, Lorenzo, Nicola Ferrara, Riccardo Basosi, and Maria Laura Parisi. 2020. "Complete Data Inventory of a Geothermal Power Plant for Robust Cradle-to-Grave Life Cycle Assessment Results." *Energies* 13(11): 2839.
Treyer, Karin, and Christian Bauer. 2016. "Life Cycle Inventories of Electricity Generation and Power Supply in Version 3 of the Ecoinvent Database—Part I: Electricity Generation." *The International Journal of Life Cycle Assessment* 21(9): 1236–54.
Uihlein, Andreas. 2018. "JRC Geothermal Power Plant Dataset: JRC Technical Reports" ed. Publications Office of the European Union. doi:10.2760/203858.
Verein Deutscher Ingenieure (VDI) (ed.). 2012. "Cumulative Energy Demand (KEA) - Terms, Definitions, Methods of Calculation." 01.040.27, 27.100(VDI 4600).
Wernet, Gregor et al. 2016. "The Ecoinvent Database Version 3 (Part I): Overview and Methodology." *The International Journal of Life Cycle Assessment* 21(9): 1218–30.
Zarrouk, Sadiq J., and Hyungsul Moon. 2014. "Efficiency of Geothermal Power Plants: A Worldwide Review." *Geothermics* 51: 142–53.

A. Annex

A.1. Evaluation model

The following changes were applied to the original model developed by (Lacirignola et al. 2014):

- Two different types of reservoir types were considered: shallow hydrothermal and deep hot rock (EGS).
- The original model uses a parameter reflecting the internal power consumption of pumps. This parameter was replaced by the internal/parasitic power consumption
- Well closing was added to the model
- The number of wells were calculated as described in section A.2.1. In the original model, the number of wells is an exogenous variable.
- The drilling success rate and additional wells required due to well depletion were included
- Emissions of NGC were included.

A.2. Key parameters and Life Cycle Inventory (LCI) of geothermal power generation

As previously described, parameter ranges are used for most important parameters to account for potential local conditions (geological characteristics, energy demand, political framework, technical developments, energy prices etc.). In the following section, the LCI and key parameters used are explained for each element contained in equations (2) to (4). All background processes and substituted products were modeled using the ecoinvent 3.7 database (consequential system model) (Wernet et al. 2016).

Please note: A statistical distribution and corresponding statistical parameters are given in parentheses for each model parameter. These distributions are applied to account for the variability of real-world conditions.

A.2.1. General parameters

A key parameter used for all components is the plants life time (LT). A lifetime of 30 years is assumed (uniform; mean 30; min 20; max 40).

A.2.2. Geothermal wells: construction, closing and enhancement

Geothermal wells are drilled using GA Drilling's Plasmabit technology. The Plasmabit technology is a plasma drilling based on the spatial rotation of an electric arc (Kocis et al. 2017). The technology is faster and requires substantially less energy than conventional contact drilling.

The model comprises GHG emissions of well drilling (GHG_{wells}), well closing ($GHG_{well\ closure}$) and well enhancement (GHG_{EGS}). These emissions are scaled in equations (2) to (4) by the number of wells (n) (all), well depths (d) (only GHG_{wells}) and, a scaling factor (SF) (only GHG_{EGS}). Table A1 lists the key parameters and formulas to estimate scaling parameters as well as the LCI of well construction, respectively. The GHG emissions of well drilling (GHG_{wells}), well closing ($GHG_{well\ closure}$) and well enhancement (GHG_{EGS}) used in equations (2) to (4) was determined using the LCI listed in Table A2 to A4.

Table A1 *Key Parameters of well construction, closing and enhancement. Abbreviations and parameter definitions according to equations (2) to (4).*

Parameter	Description
Well depth (d)	For each electrical plant type, two well types are evaluated: shallow hydrothermal and deep EGS. The assumed average well depths (d) are 2,000 and 6,000 m in case of the shallow and deep well respectively. Wide ranges are applied in the simulation to account for many possible well depths. (uniform; mean 2,000; min 1,000 max 5,000) and (uniform; mean 6,000; min 5,000; max 10,000) The well depth of direct heating is 2,500 m. (uniform; mean 2,500; min 100; max 5,000).
Number of wells (n)	The number of wells (n) was calculated according to equation (5): $n = (1 + f_{mw} + f_{IP}) * \frac{\frac{C_{SF/DF/ORC-plant}}{LF}}{W_i*(1+r)} * \frac{1}{f_{DS}}$ (5) In addition to the initial well capacity (W_i), a production reserve (r) of 10% is considered (Sanyal et al. 2014). The number of wells also depends on additional make-up wells to be drilled (f_{mw}), the drilling success rate (f_{DS}) and additional injection wells (f_{IP}) needed.
Well capacity (W_i)	Economic success and required well capacity depends on many local factors, e.g. geological features, energy demand, etc., and therefore varies in different countries and within countries among different sites. In literature minimum capacities per well are reported from as low as 3 MWe (e.g. a site in Mexico (Boissavy 2019)) to up to 9.8 MW_{el} (statistical evaluation of all power plants in Indonesia (Sanyal et al. 2014)). In the United States, the median capacity per well is 7 MWe (Lowry et al. 2017). Deep geothermal wells might require up to 10 to 20 MW_{el} to be considered viable. In future, a capacity of 30 to 50 MW_{el} per well could be achieved in favourable sites, such as Iceland or Indonesia. In Indonesia, certain wells exist that reach capacities of up to 33 MW_{el} already today (Sanyal et al. 2014). In this study, the initial well capacity of shallow wells drilled for electric geothermal plants (i.e. SF, DF and ORC) is taken from a literature review comprising 2613 geothermal wells (International Finance Corporation 2013). The review reveals a lognormal distribution of well capacities (Figure A1). (lognormal, mean 6.8, GSD 1.64)

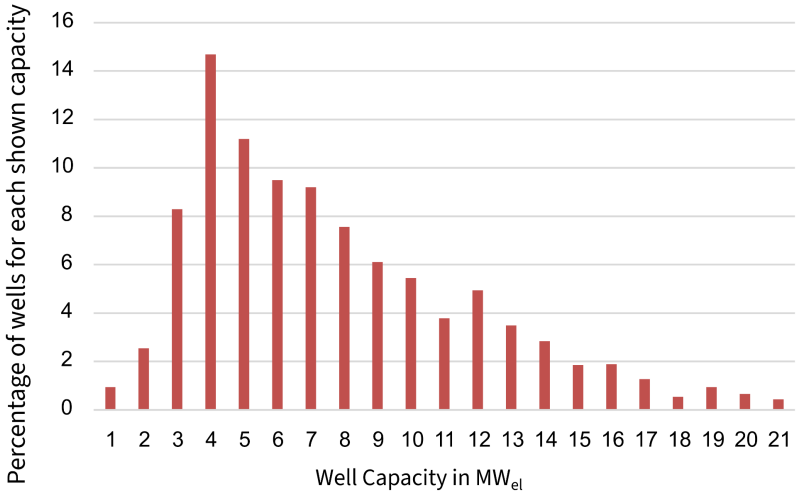

Figure A1 *Well capacity of 2613 wells. Data extracted from (International Finance Corporation 2013).*

The lognormal distribution is applied to shallow wells (<5,000 m). For deeper wells, no such distribution or statistics is currently available due to the lack of existing power plants. Therefore, well capacities of 8, 15 and 20 were assumed for SF, DF and ORC plants with deep wells (5,000 to 10,000 m), respectively. (uniform; mean 8; min 5; max 15), (uniform; mean 15; min 10; max 40) and (uniform; mean 20; min 15; max 50)

There is no comprehensive review on thermal well capacities of direct heat plants. Based on values in available studies, an average well capacity of 10 MW_{th} for direct heat use (Bakema and Schoof 2016) (uniform; mean 10; min 2; max 20).

Make-up wells (f_{mw})

Make-up wells are needed, because the well productivity W decreases over time. The well productivity at a certain point in time (t) can be calculated by equation (6) using the initial decline rate (D_i) (Sanyal et al. 2014). A decline rate of 0.04 as assumed (uniform, mean 0.04; min 0.01; max 0.07).

$$W(t) = \frac{W_i}{1+D_i*t} \quad (6)$$

The harmonic decline rate in equation (6) decreases in time and depends on the initial decline rate (D_i). Based on equation (6), the overall output of a well (P_{well}) over its lifetime (LT) can be determined by

$$P_{well} = \int_0^{LT} W(t)\,dt = \left[\frac{W_i*LN(\frac{1+D_i*t}{D_i})}{D_i}\right]_0^{LT} \quad (7)$$

A factor is calculated to compute the number of make-up wells needed (f_{mw}) per production well:

$$f_{mw} = \frac{W_i*LT}{P_{well}} - 1 \quad (8)$$

Equation (8) is a simplified approach. It neglects that towards the end of a plant's life cycle, no more makeup wells are drilled and overall production might decline.

Re-injection wells (f_{IW})

Geothermal fluid is re-injected to recharge the aquifer (in case of hydrothermal systems) or to recirculate the heat carrier medium (in case of EGS). This requires injection wells. The literature review revealed an injection to production ratio ratio ranging from ~0.3 to 2 (Tomasini-Montenegro et al. 2017; Karlsdóttir et al. 2015; Stefánsson 2002). A ratio (f_{IW}) of 1 is assumed on average. (uniform; mean 1.0; min 0.3; max 2.0)

Drilling success	The drilling success rate (f_{DS}) often increases throughout a project. Exploration wells exhibit a lower success rate than subsequently drilled wells, e.g. development and makeup wells. The success rate depends on local factors, e.g. geology. The aforementioned comprehensive review shows drilling success rates fluctuating between 65 and 80% for different depths (International Finance Corporation 2013). There is no corresponding mathematical relation apparent linking depth and success rates. It is likely that the success rate depends on a combination of well depth and local geological features. The review reports an average success rate of 78%, which is applied in this study. (uniform; mean 0.78; min 0.6; max 0.85)
Enhancement	Well enhancement is scaled by a scaling factor (SF) to account for local characteristics requiring different enhancement efforts (Lacirignola et al. 2014). The reader is referred to (Lacirignola et al. 2014) and literature therein for further details on the factor and corresponding lognormal distribution (lognormal; mean 1; GSD e[1])

***Table A2**: LCI of well drilling. Data sources (Lacirignola et al. 2014; Menberg et al. 2016). In all cases, a uniform distribution is assumed conservatively. The uncertainty is taken from (Lacirignola et al. 2014), if not otherwise specified.*

		Unit	Mean	Uncertainty	Min	Max
Inputs	Decarbonized water	kg	1110	10%	999	1221
	Salt	kg	50.5	10%	45.45	55.55
	Reinforcing steel	kg	111.3	10%	100.17	122.43
	Cement	kg	40.68	10%	36.61	44.75
	Blast furnace slag cement	kg	4.9	10%	4.41	5.39
	Chemicals inorganic	kg	2.81	10%	2.53	3.09
	Bentonite	kg	8.78	10%	7.90	9.66
	Silica sand	kg	1.52	10%	1.37	1.67
	Sodium hydroxide, 50% in water	kg	2.8	10%	2.52	03.08
	Soda powder	kg	0.6	10%	0.54	0.66
	Steel, metal working	kg	111.3	10%	100.17	122.43
	Electricity	MJ	400	50%	200	600
Output	Geothermal well	m	1			
	disposal, drilling waste, 71.5% water, to residual material landfill	kg	290	10%	261	319
	Wastes		Equivalent quantities of material inputs			

[a] The energy demand of plasma drilling under varying real-world conditions is yet not publically available. Therefore, the energy demand was estimated according to other advanced drilling technologies (Menberg et al. 2016). A wide uncertainty range was chosen to account for the lack of data.

***Table A3**: LCI of well closing (Blanc et al. 2020). In all cases, a uniform distribution is assumed conservatively. The uncertainty is taken from (Blanc et al. 2020), if not otherwise specified.*

		Unit	Mean	Uncertainty	Min	Max
Inputs	Diesel	MJ	1,075,000.00	20%	860,000.00	1,290,000.00
	Concrete	m^3	10.42	25%[a]	7.18	13.02
	Filler	kg	5000.00	25%[a]	3750.00	6250.00

[a] A conservative uncertainty range of 25% was assumed.

***Table A4**: LCI of well enhancement. Data and uncertainty ranges taken from (Lacirignola et al. 2014). In all cases, a uniform distribution is assumed conservatively.*

		Unit	Mean	Uncertainty	Min	Max
Inputs	Decarbonized water	MJ	1066000	40%	639600	1492400
	Salt	m^3	15000	40%	9000	21000
	Hydrochloric acid	kg	34470	40%	20682	48258
	Transport, lorry	tkm	7600	40%	4560	10640
	Electricity[a]	MJ	55000	40%	33000	77000

[a] The original data set assumes that diesel is used in a generator to supply electricity. In this study, it is additionally assessed how the use of grid electricity affects results.

A.2.3. Geothermal power plants

The scaling parameters used to scale geothermal power plants (equations (2) and (3)) are listed in Table A5. The LCI of geothermal power plants includes:

- The LCI of all plant components of the SF and DF plants (GHG_{OM} + $GHG_{PP,SF/DF}$) in equations (2) and (3) are listed in Tables A6 and A7. These values are scaled according to the electric capacity (MW_{el}) The LCI also separately includes collection pipelines (Table A8). The mean length of collection pipelines is 30,000 m (uniform; mean 30,000; min 10;000; max 50,000). The reported LCI of pipelines is scaled according to length.
- The LCI of all plant components of the ORC plant (GHG_{ORC}) in equations (2) and (3) are listed in Table A9 and A10.
- The LCI of all heating components are listed in Tables A11 and A12. These components are scaled according to the thermal power capacity (MW_{th})

Table A5 *Parameters of geothermal power plants. Abbreviations and parameter definitions according to equations (2) to (4).*

Parameter	Description
Plant capacity	It is assumed that future shallow geothermal power plants operating at similar depth as those today, are likely to exhibit similar capacity ranges. This is justified by the fact that it is assumed that the capacity of today's plants are mainly affected by existing geological features. Thus, plants operating at similar depth in future might be designed with technical parameters that are comparable to existing geothermal plants. Additionally, it is expected that the efficiency of the powerplant as well as other technical components is not expected to increase or change by a large extent[5]. The applied plant capacities of SF, DF and ORC plants are 30.4 MW_{el} (uniform; mean 30.4; min 0.3; max 110), 37.4 MW_{el} (uniform; mean 37.4; min 0.3; max 110) and 6.3 MW_{el} (uniform; mean 6.3; min 0.1; max 45). These values are based on existing geothermal power plants world-wide (International Energy Agency 2020). The thermal capacity of geothermal CHP plants was scaled according to existing conventional power plants (see section 2.2.2.2.)
Load factor	The reported global average load factors of SF, DF and binary electrical power plants are 0.801, 0.915 and 0.927, respectively (Zarrouk and Moon 2014). (uniform; min and max = average load factor ±5%). A global 2020 review of geothermal DH production reports global average capacity factors of 0.61, 0.405 and 0.245 in case of industrial heat provision, space heating and heat pumps, respectively (Lund and Toth 2021). A review of Dutch deep geothermal direct heat power plants reports capacity factors ranging from 0.34 to 0.98 (Bakema and Schoof 2016). The load factor of chp plants is 0.405 (uniform 0.405, min 0.2; max 0.6).

Table A6 *LCI of SF and DF power plant buildings (Karlsdóttir et al. 2015). The inventory is scaled according to the electric capacity in MW_{el}. In all cases, a uniform distribution is assumed conservatively. Abbr. DF - double flash; PE - polyethylene; PVC - polyvinyl chloride; SF - single flash, Unc. - Uncertainty.*

		SF				DF			
	Unit	Mean	Unc.	Min	Max	Mean	Unc.	Min	Max
Excavation	m^3	2165.00	10%	1948.50	2381.50	2136.00	10%	1922.40	2349.60
Inert filler	m^3	3891200.00	10%	3502080.00	4280320.00	3908800.00	10%	3517920.00	4299680.00
Steel	kg	86.00	10%	77.40	94.60	91.00	10%	81.90	100.10
Stainless steel	kg	11943.00	10%	10748.70	13137.30	13057.00	10%	11751.30	14362.70
Steel, metal working	kg	12029.00	10%	10826.10	13231.90	13148.00	10%	11833.20	14462.80
Aluminum	kg	517.00	10%	465.30	568.70	738.00	10%	664.20	811.80
Copper	kg	578.00	25%	433.50	722.50	577.00	25%	432.75	721.25
Mineral wool	kg	152.00	10%	136.80	167.20	150.00	10%	135.00	165.00
Plastic (PE)	kg	340.20	25%	255.15	425.25	356.40	25%	267.30	445.50
Plastic (PVC)	kg	226.80	25%	170.10	283.50	237.60	25%	178.20	297.00
Asphalt kg	kg	702.00	25%	526.50	877.50	729.00	25%	546.75	911.25

[5] The increase in performance of these plants cannot be predicted. In view of other uncertainties and parameter ranges assumed in this study, the effect of (slightly) increasing efficiencies is negligible (or does not at any additional accuracy to the results).

Table A7 *LCI of SF and DF power plant main machinery (Karlsdóttir et al. 2015). The inventory is scaled according to the electric capacity in MW_{el}. In all cases, a uniform distribution is assumed conservatively. Abbr. DF - double flash; SF - single flash.*

		SF				DF			
	Unit	**Mean**	**Unc.**	**Min**	**Max**	**Mean**	**Unc.**	**Min**	**Max**
Steel	kg	8616.00	5%	8185.20	9046.80	9015.00	5%	8564.25	9465.75
Stainless steel	kg	2343.00	5%	2225.85	2460.15	2114.00	5%	2008.30	2219.70
Steel, metal working	kg	10959.00	5%	10411.05	11506.95	11129.00	5%	10572.55	11685.45
Aluminum	kg	242.00	25%	181.50	302.50	255.00	25%	191.25	318.75
Copper	kg	363.00	10%	326.70	399.30	377.00	10%	339.30	414.70
Mineral wool	kg	246.00	10%	221.40	270.60	264.00	10%	237.60	290.40
Titanium	kg	523.00	5%	496.85	549.15	465.00	5%	441.75	488.25
Fiberglass reinforced plastic	kg	2116.00	25%	1587.00	2645.00	2142.00	25%	1606.50	2677.50
Transformer oil	kg	662.00	10%	595.80	728.20	683.00	10%	614.70	751.30

Table A8 *LCI of collection pipelines (Karlsdóttir et al. 2015). The inventory is scaled according to the length of collection pipelines. In all cases, a uniform distribution is assumed conservatively.*

	Unit	**Mean**	**Uncertainty**	**Min**	**Max**
Excavation	m^3	18.00	25%	13.50	22.50
Inert filler	m^3	8.30	25%	6.23	10.38
Steel	kg	197.00	25%	147.75	246.25
Steel, metal working	kg	197.00	25%	147.75	246.25
Aluminum	kg	6.20	25%	4.65	7.75
Mineral wool	kg	43.00	25%	32.25	53.75
Concrete	m^3	0.30	25%	0.23	0.38
Waste concrete	kg	720.00		540.00	900.00

Table A9 *LCI of the ORC pump infrastructure (Lacirignola et al. 2014). In all cases, a uniform distribution is assumed conservatively.*

	Unit	**Mean**	**Uncertainty**	**Min**	**Max**
Transport, lorry	tkm	132.26	20%	105.80	158.71
Reinforcing steel	kg	123.55	20%	98.84	148.26
Steel, metal working	kg	123.55	20%	98.84	148.26
Transport, oceanic freight ship	tkm	65.63	20%	52.50	78.75
Disposal of steel	kg	123.55	20%	98.84	148.26

Table A10 *LCI of the ORC pump infrastructure (Lacirignola et al. 2014). In all cases, a uniform distribution is assumed conservatively.*

	Unit	Mean	Unc.	Min	Max
Transport, lorry	tkm	7.85	20%	6.28	9.42
Reinforcing steel	kg	4.87	20%	3.9	5.84
Lubricating oil	kg	0.99	20%	0.79	1.19
Chromium steel 18/8	kg	1.69	20%	1.35	2.03
Copper	kg	0.55	20%	0.44	0.66
Propane	kg	0.005	20%	0	0.01
Phosphoric acid, industrial grade, 85% in H_2O	kg	0.55	20%	0.44	0.66
Chromium, metal working	kg	1.69	20%	1.35	2.03
Copper, metal working	kg	0.55	20%	0.44	0.66
Building, hall, steel construction	m^2	0.009	20%	0.01	0.01
Glass wool mat (mineral wool)	kg	0.011	20%	0.01	0.01
Natural gas, sweet, burned in production flare	m^3	0.002	20%	0	0
Transformer, high voltage use	units	0.01	20%	0.01	0.01
Disposal, drilling waste, 71.5% water, to residual material landfill	kg	0	20%	0	0
Disposal of hazardous waste	kg	0.55	20%	0.44	0.66
Disposal of mineral oil	kg	0.99	20%	0.79	1.19
Diesel, burned in diesel-electric generating set	MJ	58.97	20%	47.18	70.76

Table A11 *LCI of the heating station infrastructure (Karlsdóttir et al. 2015). In all cases, a uniform distribution is assumed conservatively. Abbr. PE - polyethylene.*

	Unit	Mean	Uncertainty	Min	Max
Steel	kg	192.00	25%	144.00	240.00
Stainless steel	kg	835.00	5%	793.25	876.75
Steel, metal working	kg	1027.00	0.25	937.25	1116.75
Aluminum	kg	7.00	10%	6.30	7.70
Copper	kg	6.00	25%	4.50	7.50
Copper, metal working	kg	6.00	25%	4.50	7.50
Mineral wool	kg	35.00	10%	31.50	38.50
Plastic (PE)	kg	1.10	25%	0.83	1.38

Table A12 *LCI of the construction work for hot water infrastructure (Karlsdóttir et al. 2015). In all cases, a uniform distribution is assumed conservatively.*

	Unit	Mean	Uncertainty	Min	Max
Excavation	m^3	767.00	5%	728.65	805.35
Inert filler	m^3	563.00	5%	534.85	591.15
Steel	kg	22058.00	5%	20955.10	23160.9
Stainless steel	kg	252.00	25%	189.00	315
Steel, metal working	kg	22310.00		21144.10	23475.9
Aluminum	kg	294.00	25%	220.50	367.5
Copper	kg	66.00	25%	49.50	82.5
Copper, metal working	kg	66.00	25%	49.50	82.5
Mineral wool	kg	249.00	25%	186.75	311.25
Asphalt kg	kg	1770.00	25%	1327.50	2212.5
Concrete	m^3	30.00	25%	22.50	37.5
Waste concrete	kg	72000.00		54000.00	90000

A.2.4. Non-condensable gasses

The emissions of NCG is considered using the values reported by Bayer et al. (2013). These values are derived from a literature review. These values are in line with values reported in other reviews, cf. (Fridriksson et al. 2016; Bertani and Thain 2002). Due to the high uncertainty and strong dependence on local factors, the average emission factor is applied, as recommended by (Fridriksson et al. 2016).

Table A13 *Emission of relevant NGC_l (Bayer et al. 2013).*

Compound	Emission factor in g/kWh
CO_2	122 (4 to 740)
CH_4	0.8 (0.75 to 0.85)

A.3. Additional data and information on the scenarios of geothermal power supply and the displaced conventional energy supply (section 2.4)

Figure A2 shows the energy demand of the power sector from 2019 to 2040 according to the IEA's World Energy Outlook. The scenarios were used to identify the marginal displacement of conventional energy supply.

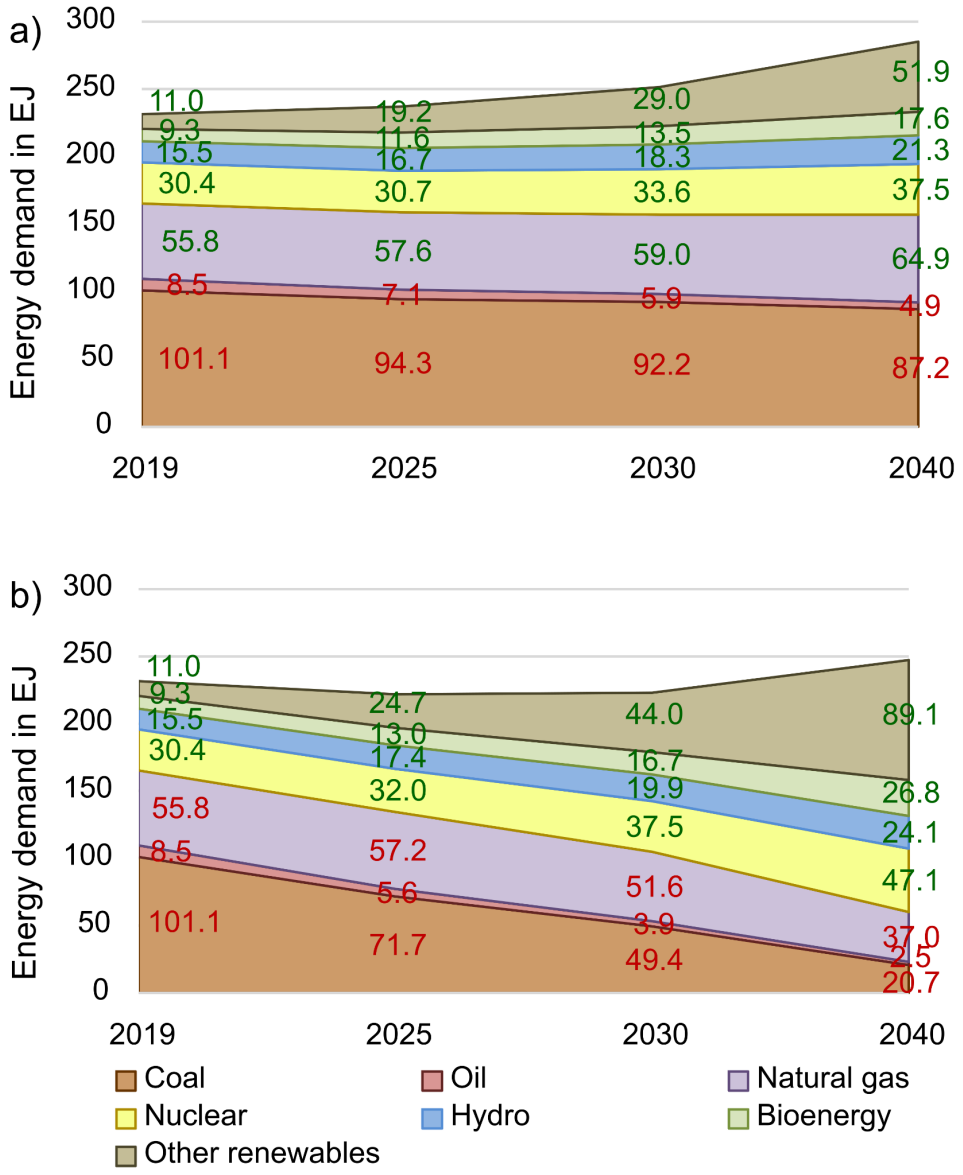

Figure A2 *Energy demand of the power sector 2019 to 2040 according to the International Energy Agency's World Energy Outlook 2020 (International Energy Agency 2020). The upper part (a) shows the Stated policy scenario. The lower part (b) shows the Sustainable development scenario. Red labels show the energy demand that decreases between 2019 and 2040 and green labels indicate an increase in the energy demand for the corresponding energy supply.*

The IEA's World Energy Outlook 2020 does not specify what type of coal is used to fulfil the demand for power generation. However, the scenarios provide a more detailed picture of coal production world-wide (for all purposes). The respective shares of hard coal and lignite were used to determine the share of hard coal and lignite used in the power generation (Table A14).

Table A14 *Absolute change in production of hard coal and lignite 2019 to 2040 and relative share of overall net decrease. Data source (International Energy Agency 2020).*

	Stated Policy		**Sustainable Development**	
	Absolute change in EJ	% of total decrease	Absolute change in EJ	% of total decrease
Hard coal	-15.11	78%	-128.70	94%
Lignite	-4.35	22%	-8.50	6%

A total of 371 data sets were evaluated (41 for lignite, 96 for hard coal, 120 for natural gas and 114 for oil) representing power generation in different countries and regions within countries (Treyer and Bauer 2016). The resulting GHG emissions and CED_f were tested with the Kolmogorov-Smirnov-Test (KS-Test) for normality and lognormality. Not all data sets' GHG emissions and CED_f followed either of these distributions. To conduct the Monte-Carlo simulation, a (pseudo-)random number generator was used to create a (pseudo-)random dataset comprising 1000 data points of those energy supplies that decrease between 2019 and 2040 in the two IEA's s energy scenarios (Tables 2 and A14). Statistical parameters for individual energy carriers and for the *Stated policy* and *Sustainable development scenarios* are shown in Tables A15 and A16.

A.4. Additional results

In the following section, additional results accompanying sections 3.1 to 3.3 are presented.

A.4.1. Additional results: Geothermal energy production (Section 3.1)

Table A15 *Mean, median, standard deviation (SD), minimum (Min.), maximum (Max.) as well as 5% and 95% percentiles (Perc.) of GHG emissions and CED_f of electricity supply from individual geothermal power plants and the supply mix without emissions of NGC. The supply mix is calculated according to the shares of each power plant type (section 2.4.1). Abbr. CED_f - cumulative fossil energy demand; D - deep well, DF - double flash; GHG - greenhouse gasses; NCG - non-condensable gasses; ORC - Organic Rankine Cycle; S - shallow well; SF - single flash.*

Indicator	Plant type	Mean	SD	Min.	Max.	Median	5% Perc.	95% Perc.
GHG emissions	SF S	29.70	20.97	4.55	368.00	24.90	10.58	63.19
g CO_2-eq./ kWh_{el}	DF S	22.10	10.46	6.18	123.00	20.00	11.03	37.69
	ORC S	32.20	12.52	11.00	110.00	29.50	17.69	55.91
	SF D	16.60	7.87	4.81	59.70	14.80	7.38	32.32
	DF D	10.80	4.73	3.58	37.70	9.70	5.35	19.70
	ORC D	5.57	3.91	0.47	40.00	4.62	1.28	13.25
	Supply mix	13.10	3.14	6.62	26.70	12.50	8.77	19.34
CED_f	SF S	0.38	0.26	0.06	4.28	0.32	0.14	0.83
MJ/ kWh_{el}	DF S	0.31	0.29	0.06	7.49	0.26	0.11	0.66
	ORC S	0.42	0.23	0.14	1.85	0.35	0.19	0.90
	SF D	0.22	0.11	0.06	0.80	0.20	0.10	0.44
	DF D	0.14	0.06	0.04	0.54	0.13	0.07	0.26
	ORC D	0.07	0.05	0.01	0.56	0.06	0.02	0.18
	Supply mix	0.17	0.04	0.09	0.39	0.17	0.11	0.26

Table A16 *Mean, median, standard deviation (SD), minimum (Min.), maximum (Max.) as well as 5% and 95% percentiles (Perc.) of GHG emissions and CED_f of heat supply from geothermal power plants without emissions of NGC. The supply mix is calculated according to the shares of each power plant type (section 2.4.1). It also includes the IEA's world energy outlook's scenarios because the heat and power capacity of CHP plants depends on displaced existing conventional base load supply. Abbr. CED_f - cumulative fossil energy demand; DF - double flash; GHG - greenhouse gasses; HC - hard coal; L - lignite; NCG - non-condensable gasses; NG - natural gas; O - oil; ORC - Organic Rankine Cycle; SF - single flash.*

Indicator	Plant type	Displacement/ Scenario	Mean	SD	Min.	Max.	Median	5% Perc.	95% Perc.
GHG emissions	SF	HC	36.80	39.70	4.30	331.50	23.80	8.60	108.40
g CO_2-eq./ kWh_{th}		L	75.00	102.20	7.30	916.70	41.10	13.90	250.40
		NG	43.30	39.90	6.50	426.90	30.20	11.50	114.60
		O	24.10	19.60	3.90	206.70	18.90	6.90	62.70
	DF	HC	27.40	28.50	4.20	295.80	18.80	6.70	81.70
		L	56.70	82.70	6.60	1,256.70	31.40	10.40	183.90
		NG	32.60	31.30	5.00	315.40	23.10	8.10	89.10
		O	17.80	13.60	3.10	120.10	14.10	5.60	44.90
	ORC	HC	15.70	19.40	1.30	215.20	9.40	2.80	47.00
		L	32.10	52.40	1.30	471.20	15.50	4.00	112.80
		NG	18.10	20.20	1.20	212.80	11.10	3.00	54.00
		O	9.80	8.40	1.20	60.20	7.10	2.20	25.90
	Supply mix	Stat. Pol.	29.20	13.00	9.70	114.30	26.40	14.40	53.50
	Supply mix	Sust. Dev.	27.80	12.60	9.50	114.50	24.70	14.10	51.20
CED_f	SF	HC	0.48	0.54	0.05	4.76	0.31	0.11	1.47
MJ/ kWh_{th}		L	0.41	0.52	0.05	4.07	0.24	0.09	1.32
		NG	0.24	0.19	0.05	1.73	0.17	0.07	0.61
		O	0.14	0.09	0.03	0.83	0.11	0.05	0.32
	DF	HC	0.15	0.14	0.03	1.50	0.11	0.05	0.46
		L	0.30	0.39	0.04	5.34	0.18	0.07	0.93
		NG	0.18	0.15	0.04	1.26	0.13	0.06	0.47
		O	0.10	0.06	0.02	0.54	0.08	0.04	0.23
	ORC	HC	0.09	0.10	0.01	0.96	0.06	0.02	0.26
		L	0.17	0.26	0.01	2.28	0.09	0.03	0.57
		NG	0.10	0.10	0.01	1.06	0.07	0.02	0.28
		O	0.06	0.04	0.01	0.32	0.05	0.02	0.15
	Supply mix	Stat. Pol.	0.22	0.12	0.07	1.06	0.19	0.10	0.42
	Supply mix	Sust. Dev.	0.22	0.13	0.07	1.20	0.18	0.10	0.43

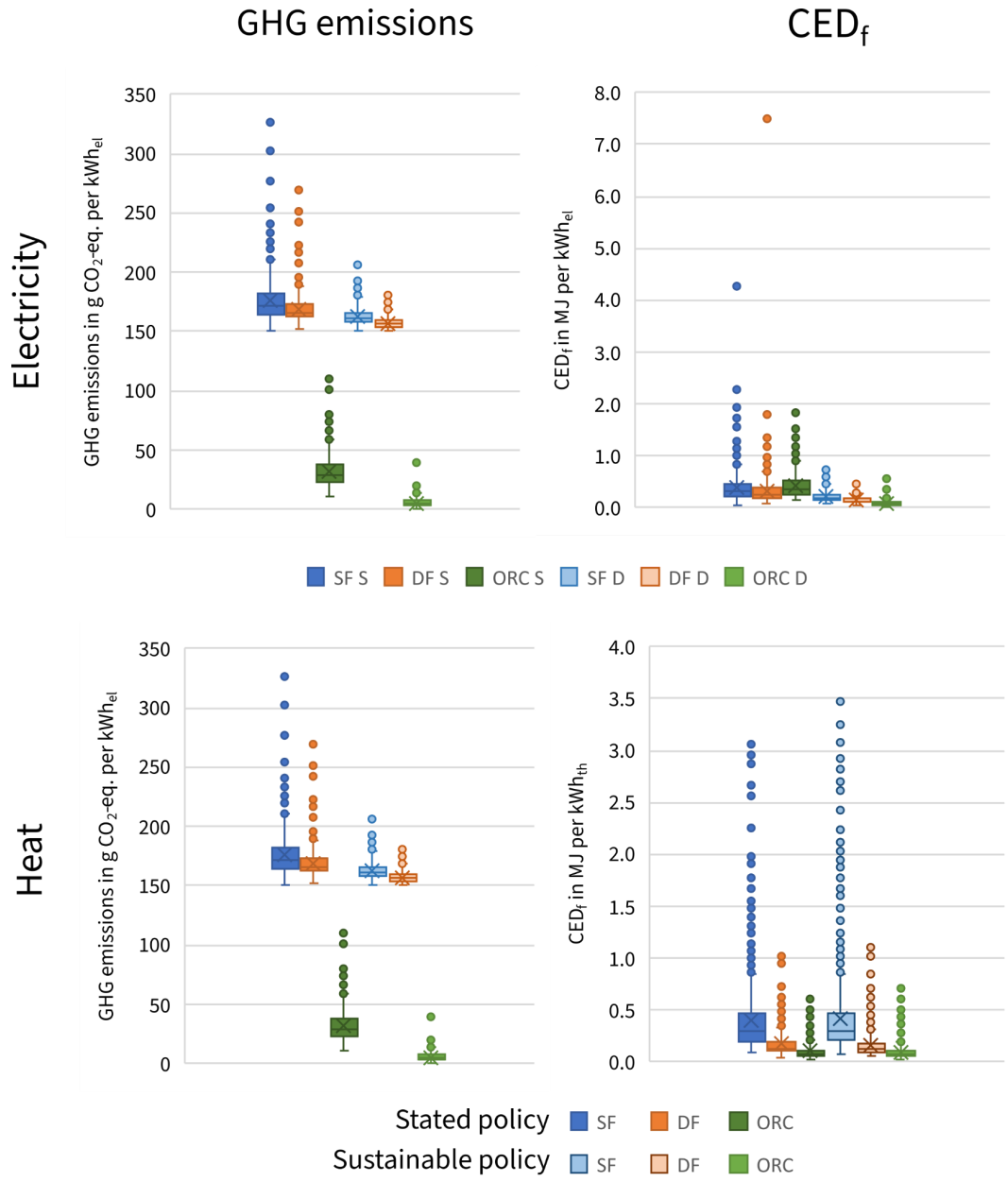

Figure A3 *Boxplots of GHG emissions and CED$_f$ of electricity and heat production. Boxplots only depict the values of geothermal power plants. Abbr. CED$_f$ - cumulative fossil energy demand; D - deep well; DF - double flash; GHG - greenhouse gasses; NCG - non-condensable gasses; ORC - Organic Rankine Cycle; S - shallow well; SF - single flash.*

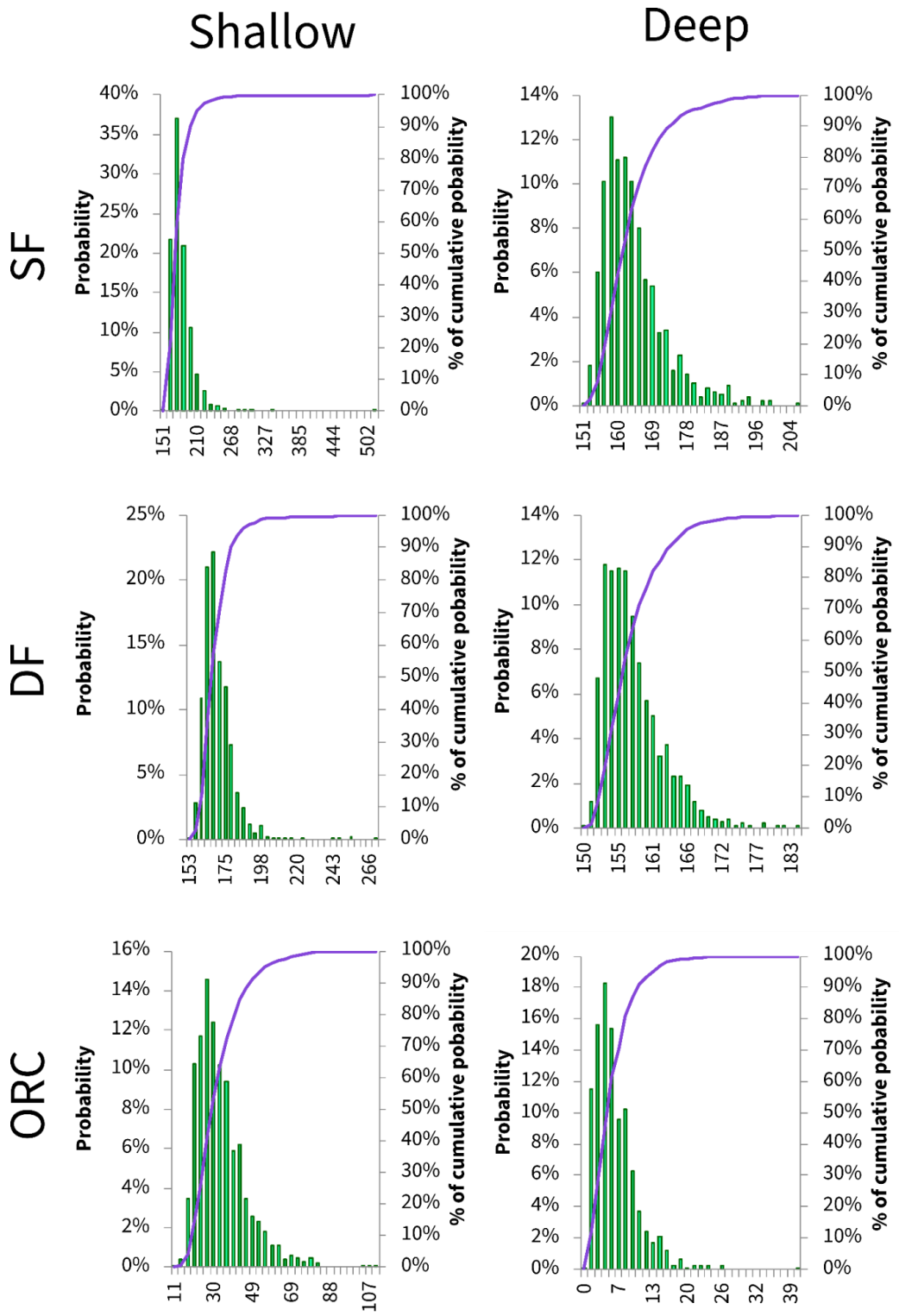

Figure A4 *Histograms of GHG emissions of geothermal electricity production. The values on the x-axes present the GHG emission classes. The GHG emissions of SF and DF include emissions of NGC. ORC plants are assumed to have no NGC. Abbr. DF - double flash; ORC - Organic Rankine Cycle; SF - single flash.*

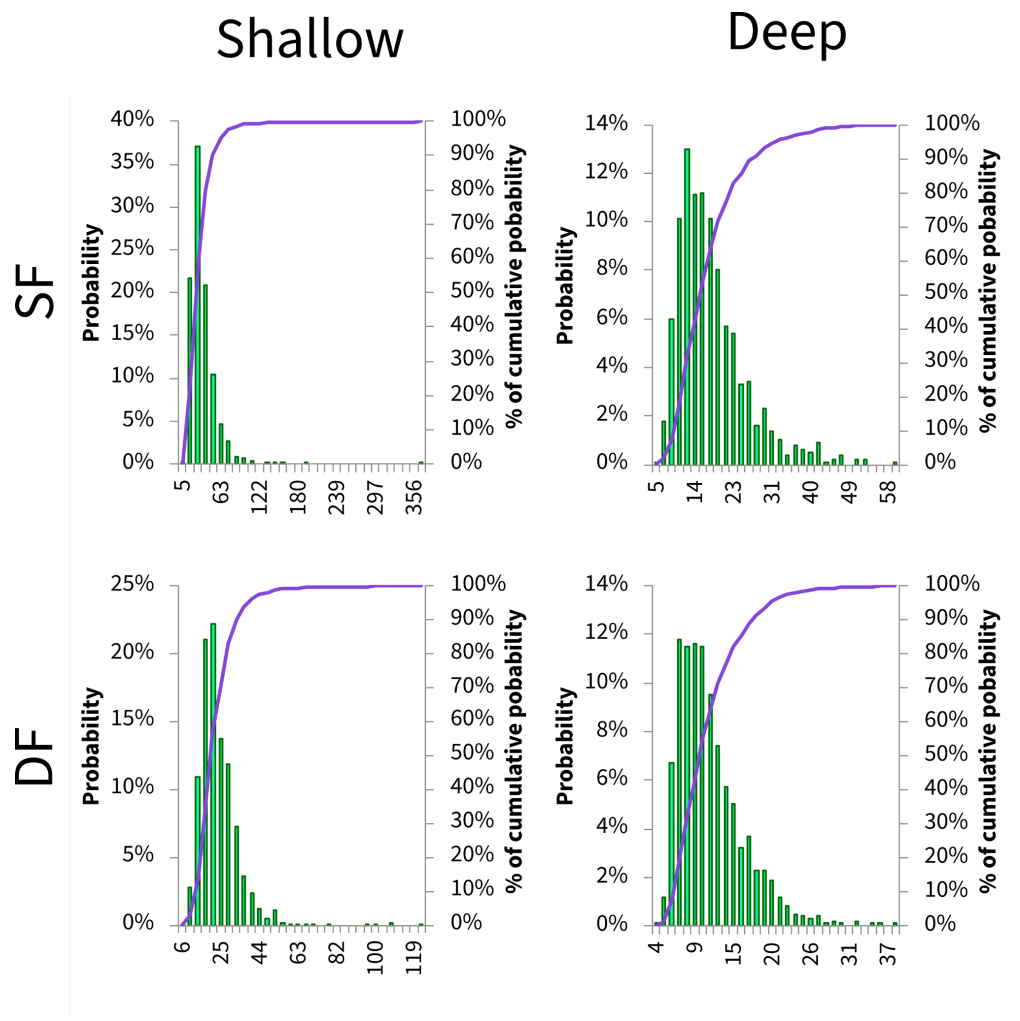

Figure A5 *Histograms of GHG emissions of geothermal electricity production without emission of NGC. The values on the x-axes present the GHG emission classes. Abbr. DF - double flash; SF - single flash.*

A.4.2. Additional results: displaced conventional energy provision (Section 3.2)

Table A17 *Mean, median, standard deviation (SD), minimum (Min.), maximum (Max.) as well as 5% and 95% percentiles (Perc.) of GHG emissions and CED_f of electricity supply from lignite, coal, natural gas, oil and according to the IEA's World Energy outlook scenarios. Abbr. CED_f - cumulative fossil energy demand; GHG - greenhouse gasses, Perc. - percentile, SD - standard deviation.*

		Mean	Median	SD	Min.	Max.	5% Perc.	95% Perc.
GHG emissions kg CO_2-eq./kWh	**Lignite**	1.27	1.23	0.17	1.03	1.79	1.07	1.69
	Hard Coal	1.27	1.22	0.23	0.93	2.01	0.99	1.75
	Natural Gas	0.54	0.51	0.14	0.35	0.96	0.37	0.84
	Oil	1.06	1.04	0.30	0.43	2.67	0.73	1.52
	Stated Policy	1.22	1.19	0.16	0.97	1.67	1.03	1.55
	Sust. Dev.	1.13	1.09	0.18	0.86	1.63	0.90	1.48
CED_f in MJ/kWh	**Lignite**	12.80	12.30	2.07	9.76	19.90	10.21	17.64
	Hard Coal	13.30	11.90	3.42	8.88	24.70	9.42	20.81
	Natural Gas	9.69	9.18	2.61	6.46	18.50	6.71	14.71
	Oil	14.30	13.80	3.87	5.86	35.50	11.00	20.19
	Stated Policy	13.30	12.60	2.34	9.66	20.60	11.00	18.42
	Sust. Dev.	12.60	11.60	2.58	8.80	21.20	10.21	17.91

Table A18 *Mean, median, standard deviation (SD), minimum (Min.), maximum (Max.) as well as 5% and 95% percentiles (Perc.) of GHG emissions and CED_f of heat provision (CHP) from lignite, coal, natural gas, oil and according to the IEA's World Energy outlook scenarios. Abbr. CED_f - cumulative fossil energy demand; GHG - greenhouse gasses, Perc. - percentile, SD - standard deviation.*

		Mean	Median	SD	Min.	Max.	5% Perc.	95% Perc.
GHG emissions	**Lignite**	2.93	3.61	1.05	0.88	3.84	0.88	3.84
kg CO_2-eq./kWh	**Hard Coal**	1.63	1.56	1.03	0.61	4.38	0.7	4.1
	Natural Gas	0.85	0.68	0.64	0.25	4.89	0.3	2.16
	Oil	0.90	0.92	0.24	0.5	1.4	0.58	1.4
	Stated Policy	1.71	1.57	0.68	0.82	3.62	0.93	3.45
	Sust. Dev.	1.51	1.41	0.77	0.72	3.75	0.79	3.46
CEDf	**Lignite**	30.5	35.57	8.94	9.09	37.7	9.09	35.83
in MJ/kWh	**Hard Coal**	15.82	13.65	9.78	6.73	48.82	6.73	36.16
	Natural Gas	17.26	11.64	14.79	1.44	91.25	4.89	44.92
	Oil	11.91	12.6	3.1	6.25	18.42	7.87	18.36
	Stated Policy	17.67	16.18	6.41	9.23	40.27	10.72	31.26
	Sust. Dev.	16.56	15.26	7.78	7.45	46.38	9	32.51

A.4.3. Additional results: Net changes in GHG emissions and CED_f (Section 3.3)

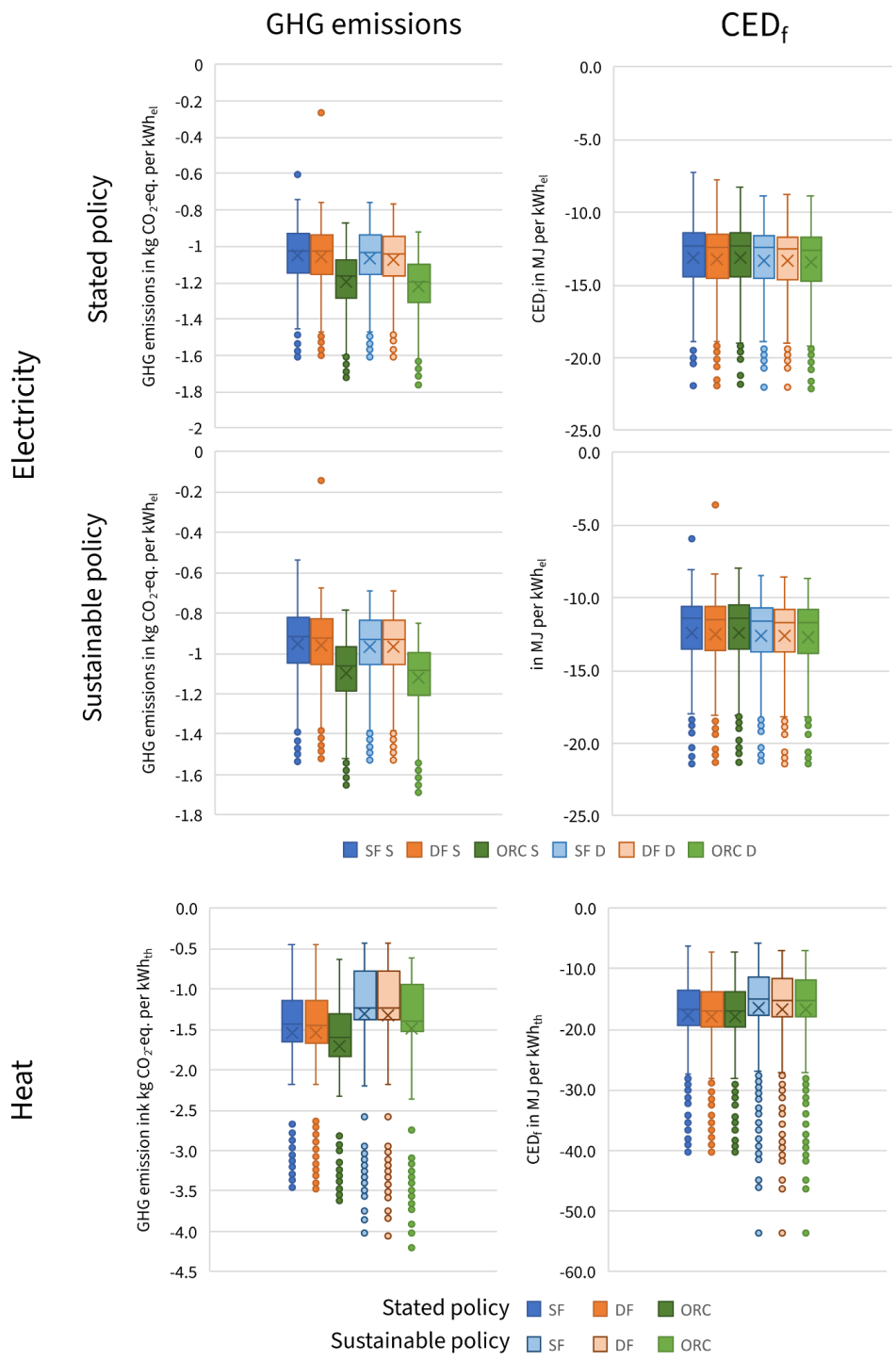

Figure A6 *Net change in GHG emissions and CED_f per kWh_{el} and kWh_{th} Abbr. CEDf - cumulative fossil energy demand; D - deep; DF - double flash; GHG - greenhouse gasses; NCG - non-condensable gasses; ORC - Organic Rankine Cycle; S - shallow; SF - single flash.*

Table A19 *Change in GHG emissions and fossil energy demand as a result of the increase in geothermal electricity production: Mean, median, standard deviation (SD), minimum (Min.), maximum (Max.) as well as 5% and 95% percentiles (Perc.). Abbr. CED_f - cumulative fossil energy demand; D - deep; DF - double flash; GHG - greenhouse gasses; NCG - non-condensable gasses; ORC - Organic Rankine Cycle; Perc. - percentile; S - shallow; SD - standard deviation, SF - single flash.*

Indicator	Scenario	Plant type	Mean	SD	Min.	Max.	Median	5% Perc.	95% Perc.
GHG emissions	**Stat. Pol.**	SF S	-1.05	0.16	-1.61	-0.60	-1.03	-1.37	-0.84
kg CO_2-eq./kWh		DF S	-1.06	0.16	-1.60	-0.27	-1.03	-1.38	-0.85
		ORC S	-1.20	0.16	-1.73	-0.87	-1.17	-1.51	-0.99
		SF D	-1.07	0.16	-1.61	-0.76	-1.04	-1.38	-0.86
		DF D	-1.07	0.16	-1.61	-0.76	-1.04	-1.38	-0.87
		ORC D	-1.22	0.16	-1.76	-0.92	-1.19	-1.54	-1.02
		Weighted mix	-1.13	0.16	-1.67	-0.82	-1.10	-1.44	-0.92
	Sust. Dev.	SF S	-0.95	0.17	-1.53	-0.54	-0.92	-1.30	-0.74
		DF S	-0.96	0.17	-1.52	-0.14	-0.93	-1.30	-0.75
		ORC S	-1.10	0.17	-1.65	-0.79	-1.06	-1.44	-0.88
		SF D	-0.97	0.17	-1.53	-0.69	-0.93	-1.31	-0.75
		DF D	-0.97	0.17	-1.54	-0.70	-0.93	-1.31	-0.76
		ORC D	-1.12	0.17	-1.69	-0.85	-1.09	-1.47	-0.92
		Weighted mix	-1.03	0.17	-1.59	-0.76	-0.99	-1.37	-0.82
CED_f	**Stat. Pol.**	SF S	-13.10	2.41	-21.90	-7.27	-12.30	-17.84	-10.35
in MJ/kWh		DF S	-13.20	2.40	-22.00	-7.77	-12.40	-17.96	-10.41
		ORC S	-13.10	2.40	-21.80	-8.28	-12.30	-17.78	-10.32
		SF D	-13.30	2.40	-22.00	-8.88	-12.50	-18.06	-10.55
		DF D	-13.40	2.39	-22.10	-8.82	-12.60	-18.08	-10.62
		ORC D	-13.40	2.39	-22.10	-8.89	-12.60	-18.19	-10.68
		Weighted mix	-13.30	2.39	-22.10	-8.81	-12.50	-18.10	-10.60
	Sust. Dev.	SF S	-12.40	2.68	-21.40	-5.98	-11.50	-17.62	-9.38
		DF S	-12.50	2.68	-21.30	-3.59	-11.50	-17.71	-9.49
		ORC S	-12.40	2.67	-21.30	-7.97	-11.40	-17.64	-9.29
		SF D	-12.60	2.67	-21.20	-8.50	-11.60	-17.84	-9.65
		DF D	-12.70	2.66	-21.40	-8.55	-11.70	-17.83	-9.69
		ORC D	-12.70	2.66	-21.50	-8.67	-11.70	-17.89	-9.72
		Weighted mix	-12.70	2.66	-21.50	-8.68	-11.80	-17.94	-9.74

Table A20 *Change in GHG emissions and fossil energy demand as a result of the increase in geothermal heat production by CHP: Mean, median, standard deviation (SD), minimum (Min.), maximum (Max.) as well as 5% and 95% percentiles (Perc.). Abbr. CED_f - cumulative fossil energy demand; D - deep; DF - double flash; GHG - greenhouse gasses; NCG - non-condensable gasses; ORC - Organic Rankine Cycle; Perc. - Percentile; S - shallow; SD - standard deviation; SF - single flash.*

Indicator	Scenario	Plant type	Mean	SD	Min.	Max.	Median	5% Perc.	95% Perc.
GHG emissions	**Stat. Pol.**	Weighted SF	-1.54	0.63	-3.45	-0.46	-1.44	-3.19	-0.78
kg CO_2-eq./kWh		Weighted DF	-1.55	0.63	-3.47	-0.45	-1.45	-3.20	-0.79
		Weighted ORC	-1.71	0.63	-3.62	-0.63	-1.61	-3.36	-0.96
		Weighted mix	-1.61	0.63	-3.52	-0.52	-1.50	-3.25	-0.87
	Sust. Dev.	Weighted SF	-1.31	0.73	-4.03	-0.44	-1.23	-3.24	-0.60
		Weighted DF	-1.32	0.73	-4.05	-0.44	-1.24	-3.25	-0.60
		Weighted ORC	-1.48	0.73	-4.20	-0.62	-1.40	-3.40	-0.76
		Weighted mix	-1.33	0.71	-3.94	-0.50	-1.25	-3.18	-0.64
CED_f	**Stat. Pol.**	Weighted SF	-17.73	6.40	-40.21	-6.16	-16.71	-31.55	-10.23
MJ/kWh		Weighted DF	-17.96	6.38	-40.19	-7.29	-16.95	-31.63	-10.58
		Weighted ORC	-18.03	6.37	-40.27	-7.21	-16.98	-31.69	-10.71
		Weighted mix	-17.91	6.38	-40.22	-7.22	-16.92	-31.60	-10.55
	Sust. Dev.	Weighted SF	-16.47	7.56	-53.59	-5.73	-15.02	-33.20	-8.58
		Weighted DF	-16.72	7.52	-53.55	-6.94	-15.29	-33.60	-8.84
		Weighted ORC	-16.79	7.52	-53.63	-6.92	-15.37	-33.65	-8.97
		Weighted mix	-16.02	7.24	-51.48	-6.47	-14.64	-32.20	-8.48

www.planet-a.com